Title: Transient Receptor Potential Melastatin 7 Cation Channel (TRPM7) Kinase: a new player in Ang II-induced hypertension

Manuscript number: HYPE201507021DR1

Author(s): Rhian Touyz, University of Glasgow
Tayze Antunes, Ottawa Hospital Research Institute
Glaucia Callera, University of Ottawa
Ying He, Ottawa Hospital Research Institute
Alvaro Yogi, National Research Council Canada
Alexey Ryazanov, Rutgers University
Lillia Ryazanova, Rutgers Univ
Alexander Zhai, University of Ottawa
Duncan Stewart, Ottawa Hospital Research Institute
Alvin Shrier, McGill University

MS: HYPE201506365D/R

Transient Receptor Potential Melastatin 7 Cation Channel (TRPM7) Kinase: a new player in Ang II-induced hypertension

Tayze T Antunes[1], Glaucia E Callera[1], Ying He[1], Alvaro Yogi[1], Alexey G Ryazanov[2], Lillia V Ryazanova[2], Alexander Zhai[3], Duncan J Stewart[3], Alvin Shrier[4],

Rhian M Touyz[1,5].

[1]Kidney Research Centre, Ottawa Hospital Research Institute, University of Ottawa, Canada; [2]Department of Pharmacology, Rutgers Robert Wood Johnson Medical School, USA; [3]Sprott Centre for Stem Cell Research and Regenerative Medicine Program, Ottawa Hospital Research Institute, University of Ottawa, Canada; [4]Department of Physiology and Groupe de Recherche Axé sur la Structure des Protéines, McGill University, Canada; [5]Institute of Cardiovascular & Medical Sciences, BHF Glasgow Cardiovascular Research Centre, University of Glasgow, UK.

Running title: TRPM7 kinase and Ang II-induced hypertension.

To whom correspondence should be addressed:

Rhian M Touyz, MD, PhD

Institute of Cardiovascular and Medical Sciences,

BHF Glasgow Cardiovascular Research Centre, University of Glasgow,

126 University Place, Glasgow, G12 8TA

Phone: + 44 (0)141 330 7775/7774, Fax: + 44 (0)141330-3360,

Email: Rhian.Touyz@glasgow.ac.uk

Abstract

Transient receptor potential melastatin 7 (TRPM7) is a bi-functional protein comprising a magnesium (Mg^{2+})/cation channel and a kinase domain. We previously demonstrated that vasoactive agents regulate vascular TRPM7. Whether TRPM7 plays a role in the pathophysiology of hypertension and associated cardiovascular dysfunction is unknown. We studied TRPM7kinase-deficient mice (TRPM7Δkinase) (heterozygous for TRPM7kinase) and wildtype (WT) mice infused with Ang II (400 ng/kg/min, 4 weeks). TRPM7kinase expression was lower in heart and aorta from TRPM7Δkinase versus WT mice, effects that were further reduced by Ang II infusion. Plasma Mg^{2+} was lower in TRPM7Δkinase versus WT mice in basal and stimulated conditions. Ang II increased blood pressure in both strains with exaggerated responses in TRPM7Δkinase versus WT groups ($p<0.05$). Acetylcholine-induced vasorelaxation was reduced in Ang II-infused TRPM7Δkinase mice, an effect associated with Akt and eNOS downregulation. Vascular VCAM-1 expression was increased in Ang II-infused TRPM7kinase-deficient mice. TRPM7 kinase targets, calpain and annexin-1, were activated by Ang II in WT but not in TRPM7Δkinase mice. Echocardiographic and histopathological analysis demonstrated cardiac hypertrophy and LV dysfunction in Ang II-treated groups. In TRPM7kinase-deficient mice, Ang II-induced cardiac functional and structural effects were amplified compared with WT counterparts. Our data demonstrate that in TRPM7Δkinase mice, Ang II-induced hypertension is exaggerated, cardiac remodelling and LV dysfunction are amplified and endothelial function is impaired. These processes are associated with hypomagnesemia, blunted TRPM7kinase expression/signaling, eNOS downregulation and pro-inflammatory vascular responses. Our findings identify TRPM7kinase as a novel player in Ang II-induced hypertension and associated vascular and target organ damage.

Key words: Blood pressure, endothelial dysfunction, TRPM, magnesium, signal transduction.

Introduction

The transient receptor potential (TRP) melastatin 7 (TRPM7) cation channel is a member of the TRP ion channel superfamily which, together with its homolog TRPM6, has the unique property of possessing a cation channel domain coupled to a cytosolic α-type serine/threonine kinase domain that comprises the carboxy-terminal region of the protein (hence also termed "chanzyme") (1, 2). While the channel domain regulates transmembrane magnesium (Mg^{2+}) influx, the kinase domain influences downstream signaling targets such as annexin-1, calpain, myosin-IIA heavy chain, Ef2-k and PLCγ2 (3-6). The kinase domain can also influence TRPM7 channel function (7). TRPM7 regulates many cellular processes including Mg^{2+} homeostasis, cell growth/apoptosis, motility, actin-myosin interaction, differentiation, and mechanosensitivity (8-10). Studies in TRPM7-deficient mice indicate that TRPM7 plays an essential role in embryonic development, kidney morphogenesis, cardiac function and systemic Mg^{2+} homeostasis (11-13). TRPM7 dysfunction has been implicated in numerous pathologies including neurodegenerative disorders, cancer and cardiovascular disease (14-18). Although the physiological and pathological significance of TRPM7 is becoming increasingly apparent, the biology of TRPM7, particularly in the cardiovascular system, still remains elusive.

We previously demonstrated that TRPM7 is expressed in the vasculature and that it is regulated by vasoactive agents, such as bradykinin, aldosterone, endothelin-1, and angiotensin II (Ang II) (19-23). Physical factors such as shear stress and flow stimulate TRPM7 activity implicating TRPM7 as a mechanotransducer in vascular cells (24, 25). TRPM7 plays an important role in modulating vascular smooth muscle cell (VSMC) Mg^{2+} homeostasis (1, 19-22, 26), a major determinant of VSMC function and vascular tone. Experimental evidence indicates that Mg^{2+} deficiency causes endothelial dysfunction, arterial remodeling and hypertension and that normalization of Mg^{2+} improves vascular function and reduces blood pressure (BP) (27).

Mechanisms regulating vascular Mg^{2+} in health and disease remain unclear but TRPM7 could be important. Aberrant TRPM7 expression/activity may contribute to impaired intracellular free Mg^{2+}

concentration ($[Mg^{2+}]_i$) and VSMC contraction, proliferation, inflammation, and fibrosis, important determinants of vascular dysfunction and remodelling in hypertension (28). In support of this 1) pro-hypertensive factors, such as Ang II and oxidative stress, regulate TRPM7 expression/activity (22, 29), 2) vascular TRPM7 is dysfunctional in spontaneously hypertensive rats (30), 3) renal TRPM7 is downregulated in aldosterone-infused mice (31), 4) pulsatile atheroprone shear stress stimulates endothelial TRPM7 expression (32), 5) TRPM7 is upregulated after renal ischemia (33), and 6) TRPM7 is implicated in vascular remodeling and inflammation induced by pressure overload (34). Moreover clinical studies showed decreased expression of TRP channels in cerebral vascular tissue from patients after hypertensive intracerebral hemorrhage (35).

The critical importance of TRPM7 is emerging from studies in which TRPM7 gene has been deleted. In cells from TRPM7-knockout mice and in cells in which siRNA is targeted to TRPM7, growth is abnormal, proliferation is arrested and cells undergo apoptosis and death (11, 12). In embryonic cardiomyocytes in which TRPM7 is disrupted, spontaneous Ca^{2+} transient firing is reduced with associated downregulation of voltage-dependent Ca^{2+} channel (36). At the whole animal level, homozygous TRPM7 kinase (Δ kinase) knockout is embryonic lethal, indicating the critical role of TRPM7 kinase for normal development (11,12,37). Heterozygous TRPM7kinase mice are viable, but exhibit signs of hypomagnesaemia.

Considering the importance of TRPM7 in the cardiovascular system, we hypothesised that TRPM7 disruption plays a role in the pathophysiology of hypertension. To address this we induced hypertension by Ang II infusion in mice deficient in TRPM7 kinase (TRPM7Δkinase) and investigated BP responses and effects on cardiac, renal, and vascular function. In addition, we explored putative molecular mechanisms underlying TRPM7kinase-dependent cardiovascular effects.

Methods

Please see supplemental text for detailed methods

Animals

Male mice, 3 months of age, mixed background (C57B6 and SV129), were studied including: wildtype ($TRPM7^{+/+}$) mice and mice heterozygous for the deletion of the TRPM7kinase domain (TRPM7Δkinase) (12). Homozygous mice were not studied because of embryonic lethality (12). Mice were infused with Ang II (osmotic minipumps, 4 weeks). Systolic BP was measured by plethysmography.

Echocardiography

Transthoracic echocardiography was performed at the end of the study (Vevo 2100 imaging system with 40-MHz transducer).

Vascular function

Vascular function of small mesenteric resistance arteries was studied by wire myography (38,39). Vessel contractility was assessed by concentration-response curves to norepinephrine (NE). Endothelium-dependent and -independent relaxation was assessed by measuring dilatory responses to acetylcholine (ACh) and diethylamine NONOate (DEA-NO) respectively in pre-contracted vessels.

Vascular structure and mechanics

Vascular structure and mechanics were studied by pressure myography (38).

Western Blotting

Total protein and membrane-enriched fractions were analyzed by immunoblotting.

Reactive Oxygen Species (ROS) Assessment

NADPHoxidase-derived $O2^{\bullet-}$ was assessed by lucigenin-enhanced chemiluminescence, hydrogen peroxide (H_2O_2) by Amplex Red, and nitric oxide (NO) by the Nitrate/Nitrite Colorimetric Assay Kit.

Statistics

Data are presented as means±SEM. Groups were compared using one-way ANOVA with Tukey's correction to compensate for multiple testing. $p<0.05$ was significant.

Results

Reduced cardiac and vascular TRPM7kinase expression in TRPM7Δkinase and Ang II-infused mice.

To analyze TRPM7kinase protein expression in mice, we first sought to investigate the specificity of the TRPM7kinase antibody. HEK cells overexpressing full length TRPM7 under the control of tetracycline (tet) and HEK cells deficient in the kinase domain (Δkinase) were used as we described, (23). Tet-on HEK cells with full length TRPM7 showed significant TRPM7 expression, while in Tet-on Δkinase cells, protein was undetectable (Fig. 1A). These findings confirmed the specificity of the antibody for TRPM7kinase. Using this antibody, we probed for TRPM7kinase in cardiac and vascular tissue in our experimental groups. TRPM7kinase expression was reduced ≈ 50% in cardiac and vascular tissue in TRPM7Δkinase mice compared to $TRPM7^{+/+}$ mice, which reflects the heterozygosity of the TRPM7Δkinase mice (Figs 1B, 1C). Ang II reduced TRPM7kinase expression in heart and aorta in both strains.

Immunohistochemical analysis demonstrated that in aorta, TRPM7kinase is expressed in both the vascular media (vascular smooth muscle cells (VSMC)) and in the endothelium (endothelial cells (EC)) (Fig. 1C). In Ang II-infused mice, TRPM7kinase expression in VSMC and ECs was reduced in WT and TRPM7kinase-deficient mice.

Morphological characteristics and biochemical analysis.

Body weight was similar between groups (Table 1). Cardiac mass was increased in Ang II-infused $TRPM7^{+/+}$ and TRPM7Δkinase mice versus controls. Ang II-induced cardiac hypertrophy was

significantly greater in TRPM7Δkinase mice versus Ang II-infused TRPM7$^{+/+}$. Renal mass was similar between vehicle-infused groups, and no kidney hypertrophy was observed in Ang II-infused group.

Biochemical analysis is summarized in Table 2. In vehicle-infused mice, plasma Mg^{2+} levels were lower in TRPM7Δkinase than WT mice. Ang II increased plasma Mg^{2+} in TRPM$^{+/+}$, but not in TRPM7Δkinase mice. Plasma urea levels and urinary albumin-creatinine ratio were increased in Ang II-infused mice, reflecting renal dysfunction. Ang II reduced plasma albumin, calcium and chloride levels only in TRPM7Δkinase mice. Urine nitrate/nitrite, marker of systemic NO production, was reduced in Ang II-infused groups versus control counterparts.

Echocardiography.

Echocardiography was performed to determine left ventricle (LV) dimensions and function (Table 3). No differences in echocardiographic measurements were observed between vehicle infused-groups. LV mass and intraventricular septum (IVS) thickness in diastole (d) were increased in Ang II-infused TRPM7$^{+/+}$ mice versus vehicle-infused counterparts. In TRPM7Δkinase mice EF and FS were significantly decreased upon Ang II infusion compared to vehicle-infused TRPM7$^{+/+}$. LV mass, LVIDd, LVID in systole (s) and LVPWd were increased in TRPM7Δkinase mice versus vehicle-infused TRPM7$^{+/+}$. In Ang II-infused TRPM7Δkinase mice there was a more pronounced decrease in EF, increase in LV mass and LVIDd than in Ang II-infused controls.

Cardiac histopathology

Cardiac hypertrophy was further analyzed histologically using hematoxylin and eosin (Supplemental Fig. 1A). Hematoxylin-eosin staining revealed that vehicle-infused TRPM7$^{+/+}$ and TRPM7Δkinase mice had similar cardiac morphology with no gross abnormalities. Ang II promoted an increase in heart size in both groups, with a greater effect in Ang II-infused TRPM7Δkinase mice, especially in the left ventricle (Supplemental Fig. 1B).

Cardiac collagen accumulation was assessed by Sirius Red staining (Supplemental Fig. 2A and table 4) and interstitial fibrosis was assessed by Masson's trichrome staining (Supplemental Fig. 2B). Hearts from vehicle-infused TRPM7$^{+/+}$ and TRPM7Δkinase mice did not exhibit collagen deposition nor fibrosis. In hearts from Ang II-infused mice there were foci of collagen deposition and interstitial fibrosis (Table 4). Perivascular collagen content and fibrosis were increased in Ang II-infused mice versus vehicle-infused controls (Supplemental Fig. 2A, 2B).

Aortic histopathology

Photomicrographs of Masson's trichrome-stained cross-sections of thoracic aorta showed that vehicle-infused TRPM7$^{+/+}$ and TRPM7Δkinase mice have similar media thickness. Ang II infusion led to a significant increase in the media thickness in both groups (Supplemental Fig. 3A, 3B). The thickening of the aortic media is evidenced by the distance between each concentric elastic lamina intermingled with the smooth muscle cell layers. A pronounced thickening of the perivascular adventitial layer was also observed in Ang II-infused groups.

BP effects of Ang II in TRPM7Δkinase mice

Figure 2 shows BP in TRPM7$^{+/+}$ and TRPM7Δkinase mice infused with vehicle or Ang II for 4 weeks. No differences in basal BP were observed between vehicle-infused groups. In Ang II-infused TRPM7$^{+/+}$ mice, BP increased gradually over 10 days at which time BP became significantly higher than vehicle-treated controls. BP remained elevated until the end of the experiment. In Ang II-infused TRPM7Δkinase mice, the onset of hypertension was rapid, occurring within 6 days of Ang II infusion. The magnitude of BP elevation by Ang II was significantly greater in TRPM7Δkinase mice versus vehicle-infused counterparts.

Effect of Ang II on vascular function in TRPM7Δkinase mice.

As shown in figure 3A, maximal Ach-induced relaxation was significantly reduced in mesenteric resistance arteries from Ang II-infused TRPM7Δkinase versus vehicle-infused TRPM7$^{+/+}$ mice.

Decreased sensitivity to Ach (pD_2) was observed in arteries from both Ang II-infused groups (Inset Fig. 3A). This impairment was specific for endothelium-dependent relaxation since arteries from Ang II-infused TRPM7$^{+/+}$ and TRPM7Δkinase mice showed similar relaxation to DEA-NO (NO donor) (Fig. 3B).

Contractile responses to NE were similar in vehicle-infused TRPM7$^{+/+}$ and TRPM7Δkinase mice (Fig. 3C). Ang II-infused mice displayed increased contraction to NE compared to vehicle-infused counterparts.

Ang II effects on vascular structure.

Pressurized arteries had comparable lumen diameter at 3 mmHg of intraluminal pressure in all four groups (Supplemental Fig. 4A). With a progressive increase of intraluminal pressure, the lumen diameter increased to a lesser degree in Ang II-infused versus vehicle-infused TRPM7$^{+/+}$ mice (Fig. 4A). Media cross-sectional area (Supplemental Fig. 4B) and media to lumen ratio (Supplemental Fig. 4C) were similar in all groups at intraluminal pressure of 3 mmHg. In response to stepwise increments of intraluminal pressure these parameters were not affected by Ang II.

Vascular mechanics.

Mesenteric resistance arteries from all groups had comparable strain (Fig. 4A) at an intraluminal pressure of 3 mmHg. In arteries from vehicle-infused groups, TRPM7Δkinase mice showed decreased stress-pressure (Fig. 4B) in response to stepwise increments of intraluminal pressure compared to TRPM7$^{+/+}$. In both Ang II treated groups, artery deformation and stress-pressure in response to stepwise increments of intraluminal pressure, were lower than in vehicle-infused TRPM7$^{+/+}$ mice. Ang II evoked a shift to the left in the stress-strain curve to an equal extent in both groups, indicating that vessels from both of the Ang II-infused groups are stiffer than vehicle-infused counterparts (Fig. 4C).

Activation of vascular eNOS, Akt and caveolin-1

To investigate putative molecular mechanism underlying endothelial dysfunction in Ang II-infused TRPM7Δkinase mice, we examined vascular expression and phosphorylation of eNOS and its upstream regulator Akt in Ang II-infused TRPM7$^{+/+}$ and TRPM7Δkinase mice. As demonstrated in figure 5A basal eNOS was similar in TRPM7$^{+/+}$ and TRPM7Δkinase mice. However, in Ang II-infused TRPM7kinase-deficient mice, eNOS levels were significantly reduced compared with vehicle- and Ang II-infused TRPM7$^{+/+}$ mice. Phosphorylation of eNOS (serine 1177, activation site) was significantly decreased in Ang II-infused TRPM7Δkinase mice versus vehicle-treated mice (Fig. 5B). Akt was phosphorylated in Ang II-infused TRPM7$^{+/+}$ but not in Ang II-infused TRPM7Δkinase mice (Fig. 5C). In membrane-enriched fractions, expression of eNOS was lower and that of caveolin-1 was higher in Ang II-infused TRPM7Δkinase mice versus control counterparts (Supplemental Fig. 5A, 5B).

Ang II effects on TRPM7 targets, mitogen-activated protein (MAP) kinases and pro-inflammatory mediators in arteries from TRPM7$^{+/+}$ and TRPM7Δkinase mice.

Upon activation, calpain and annexin-1, TRPM7 kinase downstream targets, translocate to the plasma membrane. The content of calpain and annexin in membrane-enriched fractions was evaluated as a functional index of TRPM7. As shown in figure 6 Ang II increased calpain and annexin-1 membrane content in arteries from TRPM7$^{+/+}$ mice, but failed to elicit any response in TRPM7Δkinase mice.

Expression of the VCAM-1, an adhesion molecule induced by inflammatory mediators, was significantly increased in aorta from TRPM7$^{+/-}$ mice compared to other groups (Fig. 7A).

At the molecular level, MAP kinases play a key role in vascular regulation by Ang II. We evaluated activation of vascular ERK1/2 and JNK in Ang II-infused TRPM7$^{+/+}$ and TRPM7$^{+/-}$ mice. As shown in figure 7B and supplemental figure 6 Ang II significantly increased phosphorylation of ERK1/2 and JNK in arteries from TRPM7$^{+/+}$ mice. Similar responses were observed in TRPM7Δkinase suggesting that TRPM7 kinase is not critically involved in MAP kinase activation by Ang II.

Ang II effects on systemic and vascular ROS in TRPM7$^{+/+}$ and TRPM7Δkinase mice.

The role of ROS generation by Ang II was analyzed in TRPM7$^{+/+}$ and TRPM7Δkinase mice. Plasma H_2O_2 concentration was similar between vehicle-infused TRPM7$^{+/+}$ and TRPM7Δkinase mice. Ang II had no significant effect on plasma H_2O_2 in either group (supplemental Fig. 7A and 5B). NADPH-dependent superoxide anion generation was measured in aortic homogenates by lucigenin-enhanced chemiluminescence and showed similar responses in TRPM7$^{+/+}$ and TRPM7Δkinase mice (supplemental Fig. 7C). Translocation of the Nox cytosolic subunit p47phox from the cytosol to membrane was evaluated as an index of oxidase activation. Expression of p47phox in membrane-enriched fractions was similar between groups (supplemental Fig. 7D).

Discussion

This study demonstrates a distinct cardiovascular phenotype in Ang II-infused TRPM7Δkinase mice characterised by severe hypertension, exaggerated cardiac hypertrophy, worsening of left ventricular dysfunction and persistent hypomagnesemia compared with wildtype counterparts. Associated with these changes is impaired endothelial function, downregulation of eNOS and blunted signaling through TRPM7kinase, without effect on MAP kinases or redox status. Our findings identify TRPM7kinase as a novel player in the regulation of BP and cardiovascular function and indicate that TRPM7kinase perturbations may be important in the pathophysiology of Ang II-induced hypertension and associated vascular and target organ damage (Fig. 8). Cardiac and vascular expression of TRPM7kinase was significantly downregulated by Ang II in WT and TRPM7Δkinase mice indicating an important negative interaction between these systems.

Phenotypically TRPM7Δkinase mice in basal conditions were similar to wildtype controls, except for significant hypomagnesemia, likely due to reduced intestinal Mg^{2+} absorption and increased renal Mg^{2+} wasting, since TRPM7 and its homologue TRPM6 are major Mg^{2+} transporters in epithelial cells in the gastrointestinal tract and kidneys as we reported (1-3, 12, 13). Similar to other knockout models used to interrogate the pathophysiology of hypertension, a pathological phenotype was only unmasked when TRPM7Δkinase mice were challenged with Ang II. In mice deficient in TRPM7kinase, Ang II-induced

hypertension was exaggerated and target organ damage was amplified. These phenomena were associated with pronounced endothelial dysfunction and blunted TRPM7kinase signaling through Akt, calpain and annexin-1. The relationship between reduced TRPM7 expression/activity, hypomagnesemia and BP has previously been suggested in experimental models of hypertension (16, 27, 40-42). Here we advance this concept and suggest that TRPM7kinase fine-tunes Ang II actions, because when it is downregulated, Ang II effects were augmented. This is supported by our previous findings in another mouse model with hereditary hypomagnesemia and associated downregulation of TRPM7 (42). While exact molecular mechanisms underlying the regulatory role of TRPM7 are still unclear, dampened TRPM7 signaling, as demonstrated here, may be important. However, we cannot exclude the possibility that some of the observed effects in our study may also relate to altered Mg^{2+} homeostasis and hypomagnesemia, especially since our previous studies demonstrated that alterations in TRPM7Δkinase mice were ameliorated by Mg^{2+} supplementation (12).

TRPM7 plays an important role in the regulation and function of endothelial cells as demonstrated in human umbilical vein endothelial cells, where TRPM7 deficiency leads to altered growth and migration (43). In our *in vivo* study here, endothelial function was not significantly altered by Ang II in wildtype mice but was markedly impaired in Ang II-infused TRPM7Δkinase mice as evidenced by reduced endothelium-dependent vasodilation. Reasons why Ang II did not influence endothelial function, or ROS production, in wildtype mice, as expected, are unclear but may relate, in part, to the fact that the mice studied here were of mixed genetic background, where responses to vasoactive agents are variable.

Decreased acetylcholine-induced vasorelaxation in Ang II-infused TRPM7Δkinase mice was associated with decreased eNOS phosphorylation and Akt activation and increased membrane-associated caveolin-1. Since eNOS is negatively modulated by caveolin-1, upregulation of caveolin-1 may reduce eNOS bioactivity, as previously reported (44,45). In addition blunted effects of Ang II on Akt, an upstream regulator of eNOS, may play a role in reduced eNOS activation in TRPM7Δkinase mice. These molecular processes likely contribute to dampened eNOS phosphorylation and NO generation with consequent

endothelial dysfunction and reduced vasorelaxation, important determinants of BP elevation. It is also possible that hypomagnesemia in TRPM7Δkinase mice may influence endothelial function, since decreased $[Mg^{2+}]_i$ enhances agonist-stimulated vasoconstriction and impairs vasodilation, while increased $[Mg^{2+}]_i$ is associated with vasorelaxation. These effects may occur through Mg^{2+} interactions with Ca^{2+}, or through eNOS modulation by Mg^{2+} (46).

One of the earliest indicators of endothelial inflammation is expression of adhesion molecules, such as VCAM-1, which promotes leukocyte adhesion to the endothelium and migration of macrophages through the vascular media. Increased VCAM expression has been demonstrated in atherosclerosis and hypertension and is closely associated with vascular inflammation through processes that involve activation of MAP kinases and oxidative stress. In TRPM7kinase-deficient mice, Ang II induced a significant increase in VCAM-1 expression. Molecular mechanisms underlying the inflammatory response are unclear, but may relate to decreased activation of TRPM7kinase targets, annexin-1 and calpain, which have anti-inflammatory and pro-migratory functions respectively (3, 47). Reduced annexin-1 expression and increased inflammation have been demonstrated in aortas from hypomagnesemic mice (40). We recently demonstrated that the TRPM7kinase domain, but not the TRPM7 channel domain, regulates annexin-1 and calpain signalling (23). The inflammatory and endothelial responses observed in our study appear to be independent of changes in oxidative stress or redox-sensitive MAP kinase signaling, because TRPM7kinase-deficiency had little impact on Ang II-induced phosphorylation of ERK1/2 and JNK.

The hypertensive vascular phenotype is characterised not only by endothelial dysfunction, but also by vascular remodeling (28). Previous studies demonstrated a role for TRPM7 and Mg^{2+} in vascular hypertrophy in hypertension (28,41). Here we show that in Ang II-treated mice, lumen diameter was reduced and the stress-strain relationship had a leftward shift compared with controls. Effects were similar in $TRPM7^{+/+}$ and TRPM7Δkinase mice indicating that remodeling and altered mechanics (increased stiffness) induced by Ang II are independent of TRPM7 kinase. These findings are in contrast

to those for endothelial dysfunction, which had a significant TRPM7 component, suggesting that TRPM7 kinase may be more important in endothelial than vascular smooth muscle cell regulation, at least in 3 month-old mice. Whether vascular structural changes become more apparent with aging in TRPM7Δkinase mice awaits confirmation.

TRPM7 has also been implicated in cardiac regulation and growth, since disturbed TRPM7 activity leads to abnormal cardiogenesis and impaired ventricular function (36, 37). In rat cardiomyocytes increased TRPM7 activity was involved in Ang II-induced cardiac fibrosis (48). In mouse heart and aorta, upregulation of TRPM7 channels by Ang II was associated with a proliferative phenotype of ascending aortic smooth muscle cells, an effect that was mediated through TRPM7 suppression of Pyk2-ERK1/2-Elk-1 signaling (49). Moreover cardiac arrhythmias have been linked to both up- and down-regulation of TRPM7 (35, 36). In our study, decreased TRPM7kinase activity was associated with exaggerated cardiac hypertrophy and pronounced left ventricular dysfunction in Ang II-infused mice. While this might be an adaptive response secondary to severe hypertension, it is also possible that decreased myocardial TRPM7kinase activity itself may contribute to structural and functional cardiac changes.

In conclusion, we show that in heterozygous TRPM7Δkinase mice Ang II induces an exaggerated hypertensive response, pronounced cardiac hypertrophy, and worsening of left ventricular function. Associated with these changes is endothelial dysfunction and inflammation, processes linked to blunted TRPM7kinase signaling and eNOS downregulation. Vascular remodeling and vascular MAPK activation, typically associated with Ang II-induced hypertension, were not influenced by TRPM7kinase deficiency. These observations indicate that TRPM7kinase differentially regulates vascular function in hypertension, with a primary target being the endothelium. Our findings identify TRPM7kinase as a modulator of BP regulation, which when downregulated promotes severe hypertension and worsening of cardiovascular function. Moreover, we show that Ang II is a negative regulator of TRPM7. Taken together this study defines a novel TRPM7kinase-sensitive mechanism involved in Ang II-induced hypertension and target organ damage.

Perspectives

Alterations in electrolyte status and ion transporters have been implicated in the pathophysiology of hypertension. While there is extensive data on calcium, sodium and potassium in hypertension, there is a paucity of information about magnesium and its transporters. Here we identify TRPM7, a magnesium/cation channel with kinase activity, as a regulator of magnesium homeostasis and modulator of BP regulation. Altered activity of TRPM7, particularly the kinase domain, is associated with hypomagnesemia, endothelial dysfunction, vascular inflammation, cardiac dysfunction and exaggerated pressor responses to Ang II. Our findings identify TRPM7kinase and its downstream signaling pathways as a novel paradigm in Ang II-induced hypertension. Perturbed activation of TRPM7kinase may be an important mechanism linking hypomagnesemia and cardiovascular injury in hypertension,

Acknowledgements and Source of Funding

This study was funded by a grant from the Canadian Institute of Health Research (FRN57786). This work was supported by grants from PO1 GM078195 from the National Institutes of Health (AR). RMT was supported through a Canada Research Chair/Canadian Foundation for Innovation award and a British Heart Foundation Chair (CH/12/4/29762). Dr Alex Gutsol is thanked for expert histological assistance.

Disclosures: There are no disclosures to declare.

References

1. Bates-Withers C, Sah R, Clapham DE. TRPM7, the Mg(2+) inhibited channel and kinase. Adv Exp Med Biol. 2011;704:173-183.

2. Zhang Z, Yu H, Huang J, Faouzi M, Schmitz C, Penner R, Fleig A. The TRPM6 kinase domain determines the Mg·ATP sensitivity of TRPM7/M6 heteromeric ion channels. *J Biol Chem*. 2014;289:5217-5227.

3. Dorovkov MV, Kostyukova AS, Ryazanov AG. Phosphorylation of annexin A1 by TRPM7 kinase: a switch regulating the induction of an α-helix. *Biochemistry.* 2011;50:2187-2193.

4. Perraud AL, Zhao X, Ryazanov AG, Schmitz C. The channel-kinase TRPM7 regulates phosphorylation of the translational factor eEF2 via eEF2-k. *Cell Signal.* 2011;23:586-593.

5. Su LT, Agapito MA, Li M, Simonson WT, Huttenlocher A, Habas R, Yue L, Runnels LW. TRPM7 regulates cell adhesion by controlling the calcium-dependent protease calpain. *J Biol Chem.* 2006;281:11260-11270.

6. Clark K, Middelbeek J, Lasonder E, Dulyaninova NG, Morrice NA, Ryazanov AG, Bresnick AR, Figdor CG, van Leeuwen FN. TRPM7 regulates myosin IIA filament stability and protein localization by heavy chain phosphorylation. *J Mol Biol.* 2008;378:790-803.

7. Desai BN, Krapivinsky G, Navarro B, Krapivinsky L, Carter BC, Febvay S, Delling M, Penumaka A, Ramsey IS, Manasian Y, Clapham DE. Cleavage of TRPM7 releases the kinase domain from the ion channel and regulates its participation in Fas-induced apoptosis. *Dev Cell*. 2012;22:1149-1162.

8. Numata T, Shimizu T, Okada Y. TRPM7 is a stretch- and swelling-activated cation channel involved in volume regulation in human epithelial cells. *Am J Physiol Cell Physiol.* 2007;292:C460-467.

9. Chen HC, Xie J, Zhang Z, Su LT, Yue L, Runnels LW. Blockade of TRPM7 channel activity and cell death by inhibitors of 5-lipoxygenase. *PLoS One*. 2010;5:e11161.

10. Schlingmann KP, Waldegger S, Konrad M, Chubanov V, Gudermann T. TRPM6 and TRPM7--Gatekeepers of human magnesium metabolism. *Biochim Biophys Acta.* 2007;1772:813-821.

11. Li X, Wang X, Wang Y, Li X, Huang C, Li J. Inhibition of transient receptor potential melastatin 7 (TRPM7) channel induces RA FLSs apoptosis through endoplasmic reticulum (ER) stress. *Clin Rheumatol.* 2014;33:1565-1574.

12. Ryazanova LV, Rondon LJ, Zierler S, Hu Z, Galli J, Yamaguchi TP, Mazur A, Fleig A, Ryazanov AG. TRPM7 is essential for Mg(2+) homeostasis in mammals. *Nat Commun*. 2010;1:109.

13. Jin J, Wu LJ, Jun J, Cheng X, Xu H, Andrews NC, Clapham DE. The channel kinase, TRPM7, is required for early embryonic development. *Proc Natl Acad Sci U S A.* 2012;109:E225-233.

14. Jin J, Desai BN, Navarro B, Donovan A, Andrews NC, Clapham DE. Deletion of Trpm7 disrupts embryonic development and thymopoiesis without altering Mg2+ homeostasis. *Science.* 2008;322:756-766.

15. Fleig A, Chubanov V. Trpm7. *Handb Exp Pharmacol*. 2014;222:521-546.

16. Yogi A, Callera GE, O'Connor SE, He Y, Correa JW, Tostes RC, Mazur A, Touyz RM. Dysregulation of renal transient receptor potential melastatin 6/7 but not paracellin-1 in aldosterone-induced hypertension and kidney damage in a model of hereditary hypomagnesemia. J *Hypertens*. 2011;29:1400-1410.

17. Menè P, Punzo G, Pirozzi N. TRP channels as therapeutic targets in kidney disease and hypertension. *Curr Top Med Chem*. 2013;13:386-397.

18. Park HS, Hong C, Kim BJ, So I. The Pathophysiologic Roles of TRPM7 Channel. *Korean J Physiol Pharmacol*. 2014;18:15-23.

19. Callera GE, He Y, Yogi A, Montezano AC, Paravicini T, Yao G, Touyz RM. Regulation of the novel Mg2+ transporter transient receptor potential melastatin 7 (TRPM7) cation channel by bradykinin in vascular smooth muscle cells. *J Hypertens*. 2009;27:155-166.

20. Yogi A, Callera GE, Tostes R, Touyz RM. Bradykinin regulates calpain and proinflammatory signaling through TRPM7-sensitive pathways in vascular smooth muscle cells. *Am J Physiol Regul Integr Comp Physiol.* 2009;296:R201-207.

21. Touyz RM, He Y, Montezano AC, Yao G, Chubanov V, Gudermann T, Callera GE. Differential regulation of transient receptor potential melastatin 6 and 7 cation channels by ANG II in vascular smooth muscle cells from spontaneously hypertensive rats. *Am J Physiol Regul Integr Comp Physiol.* 2006;290:R73-78.

22. He Y, Yao G, Savoia C, Touyz RM. Transient receptor potential melastatin 7 ion channels regulate magnesium homeostasis in vascular smooth muscle cells: role of angiotensin II. *Circ Res.* 2005;96:207-215.

23. Yogi A, Callera GE, O'Connor S, Antunes TT, Valinsky W, Miquel P, Montezano AC, Perraud AL, Schmitz C, Shrier A, Touyz RM. Aldosterone signaling through transient receptor potential melastatin 7 cation channel (TRPM7) and its α-kinase domain. *Cell Signal.* 2013;25:2163-2175.

24. Oancea E, Wolfe JT, Clapham DE. Functional TRPM7 channels accumulate at the plasma membrane in response to fluid flow. *Circ Res*. 2006;98:245-253.

25. Numata T, Shimizu T, Okada Y. Direct mechano-stress sensitivity of TRPM7 channel. *Cell Physiol Biochem*. 2007;19:1-8.

26. Zholos A, Johnson C, Burdyga T, Melanaphy D. TRPM channels in the vasculature. *Adv Exp Med Biol.* 2011;704:707-729.

27. Yogi A, Callera GE, Antunes TT, Tostes RC, Touyz RM. Transient receptor potential melastatin 7 (TRPM7) cation channels, magnesium and the vascular system in hypertension. *Circ J.* 2011;75:237-245.

28. Savoia C, Burger D, Nishigaki N, Montezano A, Touyz RM. Angiotensin II and the vascular phenotype in hypertension. *Expert Rev Mol Med*. 2011;13:e11.

29. Inoue H, Murayama T, Tashiro M, Sakurai T, Konishi M. Mg2+ and ATP-dependent inhibition of TRPM7 by oxidative stress. *Free Radic Biol Med.* 2014;72:257-266.

30. Yogi A, Callera GE, Antunes TT, Tostes RC, Touyz RM. Vascular biology of magnesium and its transporters in hypertension. *Magnes Res*. 2010;23:S207-215.

31. Sontia B, Montezano AC, Paravicini T, Tabet F, Touyz RM Downregulation of renal TRPM7 and increased inflammation and fibrosis in aldosterone-infused mice: effects of magnesium. *Hypertension.* 2008;51:915-921.

32. Thilo F, Vorderwülbecke BJ, Marki A, Krueger K, Liu Y, Baumunk D, Zakrzewicz A, Tepel M. Pulsatile atheroprone shear stress affects the expression of transient receptor potential channels in human endothelial cells. *Hypertension.* 2012;59:1232-1240.

33. Meng Z, Wang X, Yang Z, Xiang F. Expression of transient receptor potential melastatin 7 up-regulated in the early stage of renal ischemia-reperfusion. *Transplant Proc.* 2012;44:1206-1210.

34. Li Y, Jiang H, Ruan C, Zhong J, Gao P, Zhu D, Niu W, Guo S. The interaction of transient receptor potential melastatin 7 with macrophages promotes vascular adventitial remodeling in transverse aortic constriction rats. *Hypertens Res.* 2014;37:35-42.

35. Thilo F, Suess O, Liu Y, Tepel M. Decreased expression of transient receptor potential channels in cerebral vascular tissue from patients after hypertensive intracerebral hemorrhage. *Clin Exp Hypertens.* 2011;33:533-537.

36. Sah R, Mesirca P, Van den Boogert M, Rosen J, Mably J, Mangoni ME, Clapham DE. Ion channel-kinase TRPM7 is required for maintaining cardiac automaticity. *Proc Natl Acad Sci U S A.* 2013;110:E3037.

37. Sah R, Mesirca P, Mason X, Gibson W, Bates-Withers C, Van den Boogert M, Chaudhuri D, Pu WT, Mangoni ME, Clapham DE. Timing of myocardial trpm7 deletion during cardiogenesis variably disrupts adult ventricular function, conduction, and repolarization. *Circulation.* 2013;128:101-114.

38. Briones AM, Nguyen Dinh Cat A, Callera GE, Yogi A, Burger D, He Y, Corrêa JW, Gagnon AM, Gomez-Sanchez CE, Gomez-Sanchez EP, Sorisky A, Ooi TC, Ruzicka M, Burns KD, Touyz RM. Adipocytes produce aldosterone through calcineurin-dependent

signaling pathways: implications in diabetes mellitus-associated obesity and vascular dysfunction. *Hypertension.* 2012;59:1069-1078.

39. Endemann D, Touyz RM, Li JS, Deng LY, Schiffrin EL. Altered angiotensin II-induced small artery contraction during the development of hypertension in spontaneously hypertensive rats. *Am J Hypertens*. 1999;12:716-723.

40. Paravicini TM, Yogi A, Mazur A, Touyz RM. Dysregulation of vascular TRPM7 and annexin-1 is associated with endothelial dysfunction in inherited hypomagnesemia. *Hypertension*. 2009;53:423-429.

41. Touyz RM. Transient receptor potential melastatin 6 and 7 channels, magnesium transport, and vascular biology: implications in hypertension. *Am J Physiol Heart Circ Physiol.* 2008;294:H1103-1118.

42. Baldoli E, Maier JA. Silencing TRPM7 mimics the effects of magnesium deficiency in human microvascular endothelial cells. *Angiogenesis.* 2012;15:47-57.

43. Baldoli E, Castiglioni S, Maier JA. Regulation and function of TRPM7 in human endothelial cells: TRPM7 as a potential novel regulator of endothelial function. *PLoS One.* 2013;8(3):e5989.

44. Howard AB, Alexander RW, Taylor WR. Effects of magnesium on nitric oxide synthase activity in endothelial cells. *Am J Physiol*. 1995;269:C612-618.

45. Goligorsky MS, Li H, Brodsky S, Chen J.Relationships between caveolae and eNOS: everything in proximity and the proximity of everything. *Am J Physiol Renal Physiol*. 2002;283:F1-10.

46. Basralı F, Koçer G, Ülker Karadamar P, Nasırcılar Ülker S, Satı L, Özen N, Özyurt D,

Şentürk ÜK. Effect of magnesium supplementation on blood pressure and vascular reactivity in nitric oxide synthase inhibition-induced hypertension model. *Clin Exp Hypertens.* 2015;37:1-10.

47. Su LT, Chen HC, González-Pagán O, Overton JD, Xie J, Yue L, Runnels LW. TRPM7 activates m-calpain by stress-dependent stimulation of p38 MAPK and c-Jun N-terminal kinase. *J Mol Biol.* 2010;396:858-869.

48. Yu Y, Chen S, Xiao C, Jia Y, Guo J, Jiang J, Liu P. TRPM7 is involved in angiotensin II induced cardiac fibrosis development by mediating calcium and magnesium influx. *Cell Calcium.* 2014;55:252-260.

49. Zhang Z, Wang M, Fan XH, Chen JH, Guan YY, Tang YB. Upregulation of TRPM7 channels by angiotensin II triggers phenotypic switching of vascular smooth muscle cells of ascending aorta. *Circ Res*. 2012;111:1137-1146.

Novelty and Significance

What Is New?

- TRPM7, a unique Mg^{2+} transporter with kinase activity, influences vascular function and blood pressure in Ang II-induced hypertension.
- TRPM7 kinase deficiency leads to exaggerated hypertension with associated eNOS downregulation and amplified endothelial dysfunction.
- TRPM7 kinase/eNOS is a novel system through which Ang II signals.

What Is Relevant?

- Clinical hypertension is associated with perturbed Mg^{2+} homeostasis and vascular dysfunction, possibly through TRPM7 dysfunction.
- Targeting TRPM7 kinase may have potential as a novel therapeutic target in hypertension.

Summary

TRPM7 kinase regulates vascular function in hypertension, with a primary target being the endothelium. TRPM7 kinase may have vasoprotective functions, which when dysregulated contributes to endothelial dysfunction, vascular inflammation and hypertension. We identify a novel TRPM7 kinase-sensitive mechanism in Ang II-induced hypertension.

Figure legends

Figure 1. TRPM7kinase expression in heart and aorta of TRPM7+/+ and TRPM7Δkinase mice. A. Validation of TRPM7kinase antibody (Epitomics; # 3828-1). TRPM7 kinase expression in HEK cells expressing TRPM7 full length protein (WT) and TRPM7 lacking the kinase domain (Δ kinase) under the control of tetracycline. Cells deficient in TRPM7kinase failed to express the protein. B. Hearts were isolated from $TRPM7^{+/+}$ and TRPM7Δkinase mice infused with vehicle or Ang II. Protein expression of TRPM7kinase was analyzed as a ratio to β-actin. Upper panels, representative immunoblots of TRPM7 and β-actin. Bar graphs represent mean ± SEM of 9-11 mice per group. *$p<0.05$ vs vehicle-infused $TRPM7^{+/+}$. C. TRPM7kinase expression was analyzed in aortas from vehicle and Ang II-infused mice. Panels are representative photomicrographs of paraffin-embedded aortic sections processed for immunohistochemistry of TRPM7kinase, with original magnification of x100. Data were obtained from 5 mice/group. Stars (*) and arrows (↑) indicate the presence of TRPM7kinase in vascular media and endothelium respectively.

Figure 2. Systolic blood pressure (BP) in $TRPM7^{+/+}$ and $TRPM7^{+/-}$ mice infused with Ang II. $TRPM7^{+/+}$ and $TRPM7^{+/-}$ mice were infused with vehicle or Ang II (400 ng/Kg/min., osmotic minipumps; 4 weeks). BP was measured weekly for 4 weeks (W) by tail-cuff plethysmography. Line graphs represent mean ± SEM of 10-19 mice per group. *$p<0.05$ vs vehicle-infused counterparts: $^{+}p<0.05$ vs Ang II-infused $TRPM7^{+/+}$.

Figure 3. Functional responses in mesenteric arteries from Ang II-infused $TRPM7^{+/+}$ and $TRPM7^{+/-}$ mice. Mesenteric arteries were isolated from $TRPM7^{+/+}$ and $TRPM7^{+/-}$ mice infused with vehicle or Ang II. Concentration-response curves to cumulative concentrations of acetylcholine (Ach, 10^{-9}- 3 x 10^{-5} M) (A), diethylamine NONOate (DEA-NO, 10^{-9}- 3 x 10^{-5} M)

(B), and norepinephrine (NE, 10^{-9}- 3 x 10^{-5} M) (C) were analyzed in vessels mounted on wire myographs. Line graphs represent mean ± SEM of 7- 17 mice per group. Inset (A) shows the sensitivity to Ach expressed by pD2 values. *p<0.05 vs vehicle-infused counterparts: $^{+}$p<0.05 vs Ang II-infused TRPM7$^{+/+}$.

Figure 4. Mechanical properties in mesenteric resistance arteries from Ang II-infused mice. Mesenteric resistance arteries were isolated from TRPM7$^{+/+}$ and TRPM7$^{+/-}$ mice infused with vehicle or Ang II. Strain (A), Stress (B), and Stress-strain relationship curves (C) were analyzed by pressure myography. Mesenteric arteries were incubated in 0 Ca^{2+}-physiological salt solution containing 10 mmol/L EGTA and were subjected to increasing levels of intraluminal pressure. Line graphs represent mean ± SEM of 5 mice per group. *p<0.05 vs vehicle-infused counterparts; †p<0.05 vehicle-infused TRPM7$^{+/-}$

Figure 5. Ang II effects on expression and phosphorylation of eNOS and Akt in aorta from TRPM7$^{+/+}$ and TRPM7$^{+/-}$ mice. Representative immunoblots and bar graphs of eNOS content (A), eNOS (B) and Akt (C) phosphorylation in vessels from vehicle- and Ang II-infused TRPM7$^{+/+}$ and TRPM7$^{+/-}$ mice. Levels of total eNOS, phospho eNOS and phospho Akt are expressed relative to expression of □ actin. Results are presented as mean ±□SEM of 8-9 mice per group. *p<0.05 vs vehicle-treated groups; + p<0.05 vs Ang II-infused TRPM7$^{+/+}$ mice.

Figure 6. Expression of TRPM7 kinase targets calpain and annexin-1 in membrane-enriched fractions of mesenteric arteries from Ang II-infused TRPM7$^{+/+}$ and TRPM7Δkinase mice. Mesenteric arteries were isolated from TRPM7$^{+/+}$ and TRPM7Δkinase mice infused with vehicle or Ang II. Protein content of calpain (A) and annexin-1 (B) was measured in membrane-enriched fractions. Data are presented as the expression of calpain or annexin-1 relative to the expression of β-actin. Upper panels, representative immunoblots of

calpain, annexin-1 and α actin. Results are presented as mean ±SEM of 6-9 mice per group. *$p<0.05$ vs vehicle-infused $TRPM7^{+/+}$.

Figure 7. Expression of VCAM-1 and ERK1/2 in vessels from Ang II-infused $TRPM7^{+/+}$ and TRPM7Δkinase mice. Aortas were isolated from $TRPM7^{+/+}$ and TRPM7Δkinase mice infused with vehicle or Ang II. (A) Upper panels, representative immunoblots of VCAM-1 and β-actin. Data are presented as the expression of VCAM-1 relative to the expression of β-actin. (B) Phosphorylation levels of ERK1/2 are presented relative to expression of β-actin. Upper panels, representative immunoblots of phospho-ERK1/2 and β-actin. Results are presented as mean ±SEM of 5-9 mice per group. $^{*}p<0.05$ vs vehicle infused counterparts; $^{+}p<0.05$ vs Ang II-infused $TRPM7^{+/+}$.

Figure 8. Possible molecular mechanisms whereby TRPM7 kinase deficiency amplifies Ang II cardiovascular and blood pressure (BP) effects. Blunted TRPM7 kinase signaling by Ang II through its G protein-coupled receptor is associated with reduced activation of TRPM7 kinase downstream targets, including Akt, calpain and annexin-1, leading to vascular and cardiac dysfunction and amplified increase in BP. These processes may also be influenced by reduced intracellular Mg^{2+}, possibly due to decreased transmembrane Mg^{2+} transport as a consequence of TRPM7 kinase downregulation (as we previously demonstrated (1)). (–) denotes inhibitory effect. Dashed lines are possible pathways.

Table 1. Body weight, kidney and heart mass of vehicle and Ang II-infused TRPM7$^{+/+}$ and TRPM7Δkinase mice.

Morphological Parameter	TRPM7$^{+/+}$ vehicle	TRPM7$^{+/+}$ Ang II	TRPM7Δkinase vehicle	TRPM7Δkinase Ang II
BW (g)	24.8 ± 0.7	25.5 ± 1.0	23.4 ± 0.7	24.2 ± 1.0
HM (mg)/BW(g)	4.4 ± 0.1	5.4 ± 0.1*	4.5 ± 0.1	5.8 ± 0.1*†
KM (mg)/BW(g)	6.1 ± 0.2	5.8 ± 0.1	6.2 ± 0.1	6.2 ± 0.1

TRPM7$^{+/+}$ and TRPM7Δkinase mice were infused with vehicle or Ang II (400 ng/Kg/min, 4 weeks). Results are mean ± SEM. n=6-16 mice per group. Body weight (BW), heart mass (HM), kidney mass (KM). *$p<0.05$ versus vehicle counterparts; $^{\dagger}p<0.05$ versus Ang II-infused TRPM7$^{+/+}$.

Table 2. Plasma and urine profile in vehicle- and Ang II- infused TRPM7$^{+/+}$ and TRPM7Δkinase mice.

Plasma	TRPM7$^{+/+}$ vehicle	TRPM7$^{+/+}$ Ang II	TRPM7Δkinase vehicle	TRPM7Δkinase Ang II
Total protein	44.1 ± 0.7	41.4 ± 0.9 *	43.2 ± 0.9	39.8 ±1.2 *
Albumin	6.0 ± 0.4	5.2 ± 0.5	6.2 ± 0.7	4.4 ± 0.3 *
Cholesterol	2.3 ± 0.07	2.4 ± 0.09	2.2 ± 0.06	2.2 ± 0.07
Triglycerides	1.5 ± 0.1	1.2 ± 0.1	1.3 ± 0.1	1.9 ± 0.4
Glucose	11.2 ± 0.5	11.2 ± 0.4	10.5 ± 0.5	10.5 ± 0.6
Urea	7.9 ± 0.2	11.2 ± 0.7 *	7.9 ± 0.4	10.6 ± 0.5 *
Creatinine	14.9 ± 0.9	14.0 ± 0.8	13.0 ± 1.3	12.3 ± 1.0
Calcium	1.51 ± 0.04	1.55 ± 0.06	1.46 ± 0.06	1.28 ± 0.08 *
Chloride	96.8 ± 1.2	92.8 ± 1.9	95.0 ± 1.2	88.7 ± 2.4 *
Phosphorus	1.2 ± 0.04	1.2 ± 0.07	1.1 ± 0.07	1.2 ± 0.06
Bicarbonate	19.1 ± 0.4	26.5 ± 0.5	20.0 ± 1.1	20.9 ± 1.7
Magnesium	0.65 ± 0.02	0.74 ± 0.04*	0.60 ± 0.01‡	0.64 ± 0.02†
Urine				
Albumin:creatinine ratio (µg/mg)	25 ± 6	394 ± 99*	47 ± 11	449 ± 118*
Nitric oxide (µM)	3.7 ± 0.2	3.0 ± 0.2*	3.9 ± 0.2	3.2 ± 0.1*

TRPM7$^{+/+}$ and TRPM7Δkinase mice were infused with vehicle or Ang II (400 ng/Kg/min, 4 weeks). Results are mean ± SEM. n=6-16 mice per group. *$p<0.05$ versus vehicle-treated counterparts. †$p<0.05$ versus Ang II-infused TRPM7$^{+/+}$. ‡$p<0.05$ versus vehicle-treated TRPM7$^{+/+}$

Table 3. Echocardiographic measurements from M-mode images of vehicle- and Ang II-infused TRPM7$^{+/+}$ and TRPM7Δkinase mice.

Echocardiographic Parameter	TRPM7$^{+/+}$ vehicle	TRPM7$^{+/+}$ Ang II	TRPM7Δkinase vehicle	TRPM7Δkinase Ang II
EF (%)	49.9 ± 5.5	43.6 ± 7.2	42.8 ± 3.1	22.9 ± 3.7 *†
FS (%)	25.1 ± 3.3	19.8 ± 4.3	21.6 ± 1.7	10.5 ± 1.9 *
LV mass (mg)	89.9 ± 3.4	127.1 ± 10.2 *	105.7 ± 5.9	160.9 ± 8.3 *†
IVS; d (mm)	0.77 ± 0.06	1.03 ± 0.03 *	0.89 ± 0.04	0.94 ± 0.04
LVID; d (mm)	3.6 ± 0.07	3.6 ± 0.18	3.6 ± 0.10	4.13 ± 0.15 *†
LVID; s (mm)	2.7 ± 0.1	3.1 ± 0.2	2.9 ± 0.1	3.7 ± 0.2 *
LVPW; d (mm)	0.76 ± 0.04	0.9 ± 0.03	0.79 ± 0.05	0.96 ± 0.05 *
Heart rate (bpm)	501 ± 20	472 ± 15	455 ± 13	474 ± 23

TRPM7$^{+/+}$ and TRPM7Δkinase mice were infused with vehicle or Ang II (400 ng/Kg/min., osmotic minipumps, 4 weeks). EF = Ejection fraction, FS = Fractional shortening, LV= Left ventricle, IVS = Interventricular septum, LVID = Left ventricle internal diameter, LVPW= Left ventricle posterior wall, d= in diastole, s= in systole, bpm= beats per minute. Results are mean ± SEM. n=5-10 mice per group. *p<0.05 vs vehicle-treated counterparts; †p<0.05 vs Ang II-infused TRPM7$^{+/+}$.

Table 4. Scores for collagen accumulation and fibrosis of vehicle- and Ang II- infused TRPM7$^{+/+}$ and TRPM7Δkinase mice.

	Sirius Red				Masson's Trichrome			
	-	+	++	+++	-	+	++	+++
Experimental Group								
TRPM7$^{+/+}$ Vehicle	8	0	0	0	8	0	0	0
TRPM7$^{+/+}$ Ang II	0	2	4	1	0	1	4	2
TRPM7Δkinase Vehicle	9	0	0	0	9	0	0	0
TRPM7Δkinase Ang II	0	2	3	2	0	1	5	2

Hearts were isolated from TRPM7$^{+/+}$ and TRPM7Δkinase mice infused with vehicle or Ang II (400 ng/Kg/min., osmotic minipumps, 4 weeks). Paraffin-embedded of heart sections were processed for Sirius Red (collagen) and Masson's trichrome (fibrosis). Staining for both collagen content and fibrosis were scored according to the following: – indicates intact; +, mild, ++, moderate, +++, severe. Values are numbers of mice displaying collagen deposition or fibrosis. n= 8-9 mice per group.

Figure 1

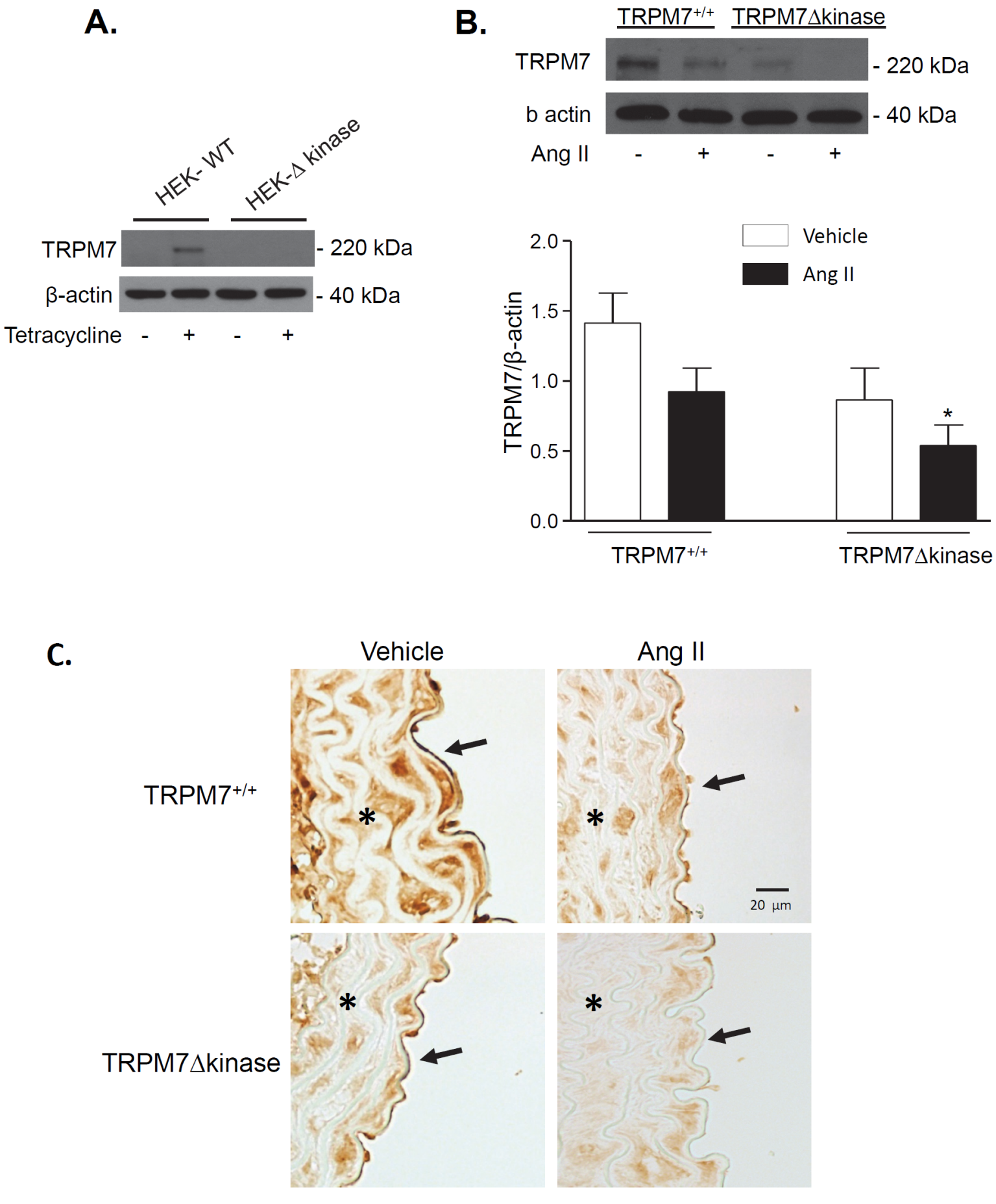
A.
HEK- WT
HEK-Δ kinase
TRPM7
- 220 kDa
β-actin
- 40 kDa
Tetracycline - + - +
B.
TRPM7+/+
TRPM7Δkinase
TRPM7
- 220 kDa
b actin
- 40 kDa
Ang II - + - +
Vehicle
Ang II
TRPM7/β-actin
2.0
1.5
1.0
0.5
0.0
*
TRPM7+/+
TRPM7Δkinase
C.
Vehicle
Ang II
TRPM7+/+
TRPM7Δkinase
20 μm

Figure 2

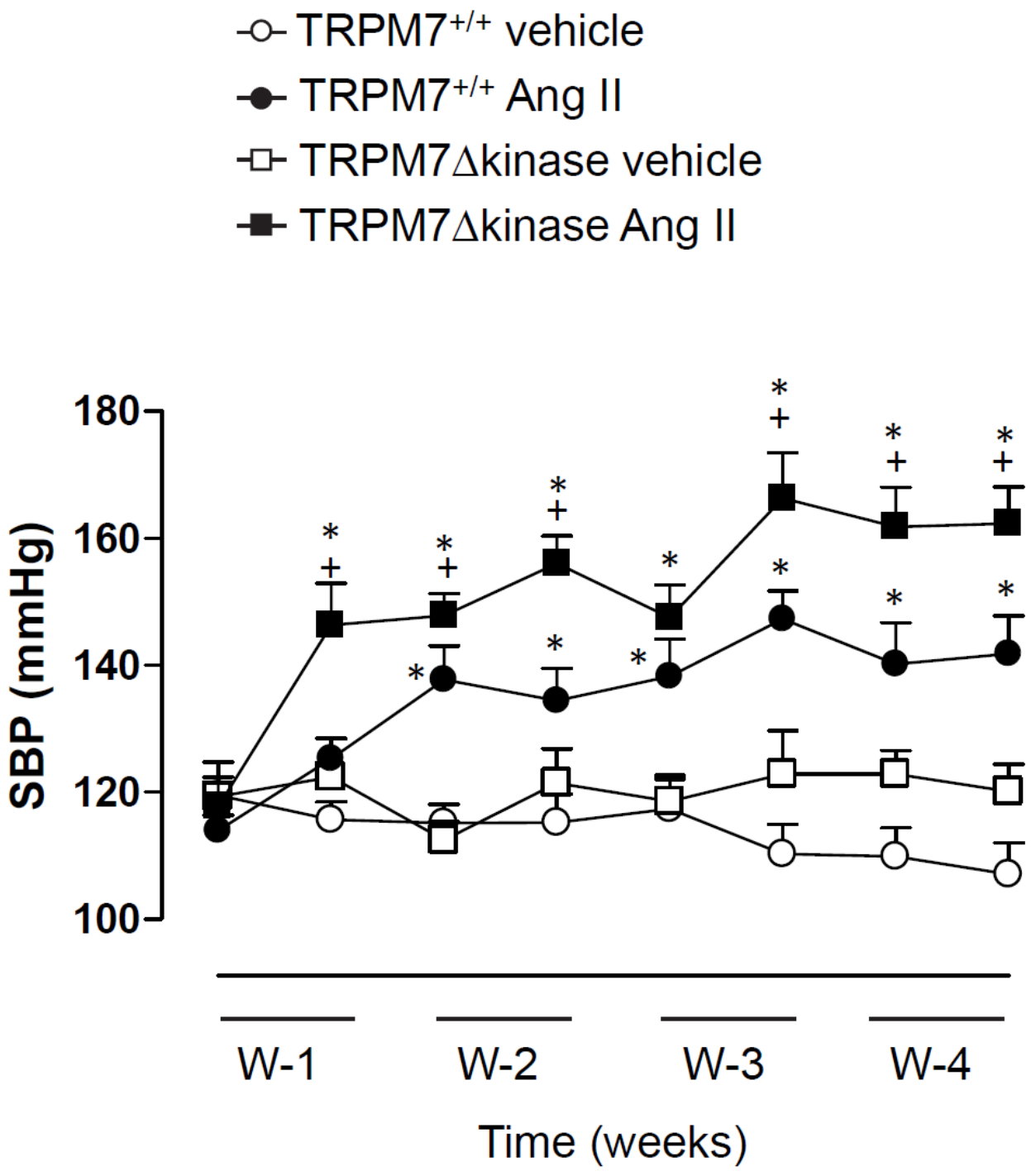
TRPM7+/+ vehicle
TRPM7+/+ Ang II
TRPM7Δkinase vehicle
TRPM7Δkinase Ang II
SBP (mmHg)
180
160
140
120
100
W-1
W-2
W-3
W-4
Time (weeks)

Figure 3

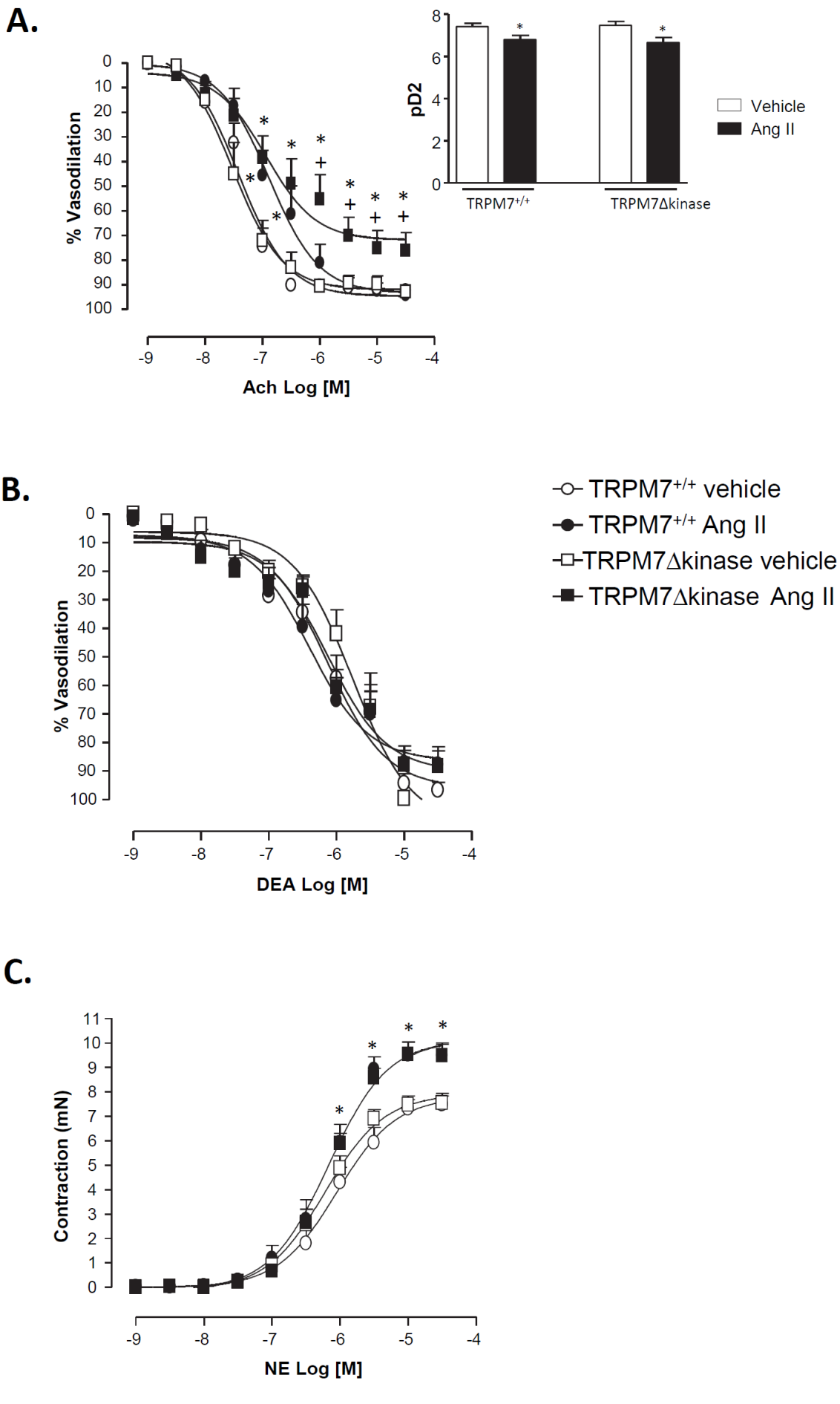
A.
% Vasodilation
Ach Log [M]
pD2
TRPM7+/+
TRPM7Δkinase
Vehicle
Ang II
B.
% Vasodilation
DEA Log [M]
TRPM7+/+ vehicle
TRPM7+/+ Ang II
TRPM7Δkinase vehicle
TRPM7Δkinase Ang II
C.
Contraction (mN)
NE Log [M]

Figure 4

A.

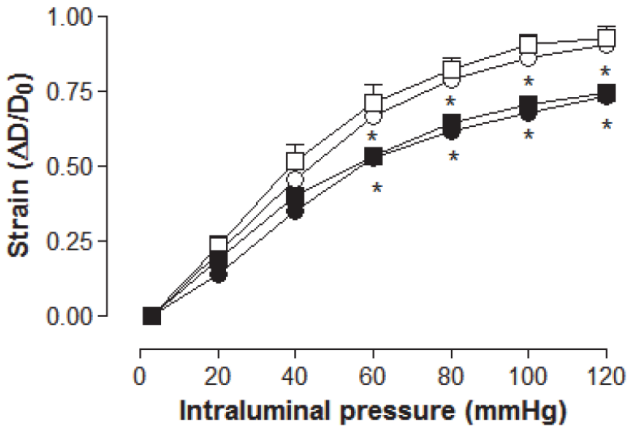
Strain (ΔD/D0)
1.00
0.75
0.50
0.25
0.00
0
20
40
60
80
100
120
Intraluminal pressure (mmHg)

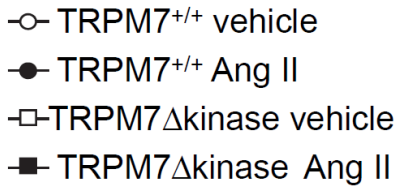
TRPM7+/+ vehicle
TRPM7+/+ Ang II
TRPM7Δkinase vehicle
TRPM7Δkinase Ang II

B.

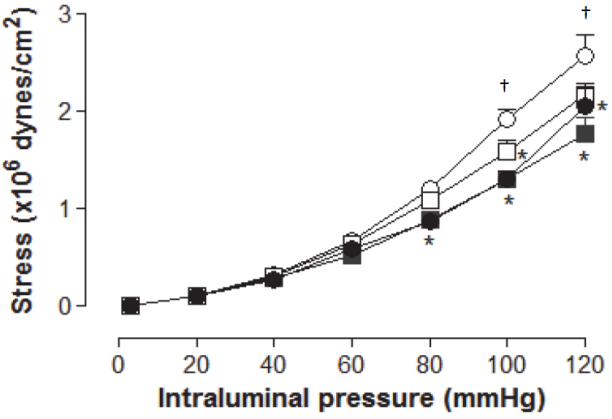
Stress (x10^6 dynes/cm^2)
3
2
1
0
0
20
40
60
80
100
120
Intraluminal pressure (mmHg)

C.

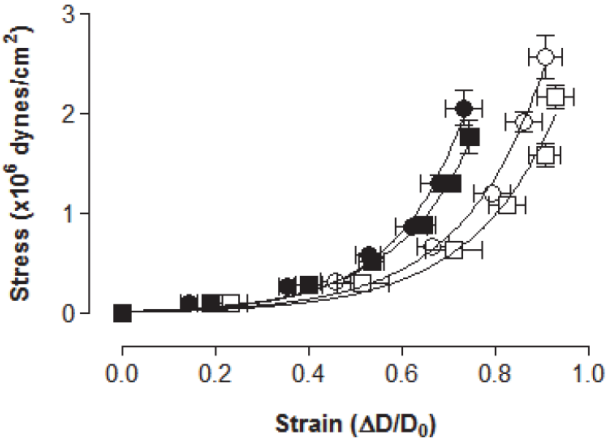
Stress (x10^6 dynes/cm^2)
3
2
1
0
0.0
0.2
0.4
0.6
0.8
1.0
Strain (ΔD/D0)

Figure 5

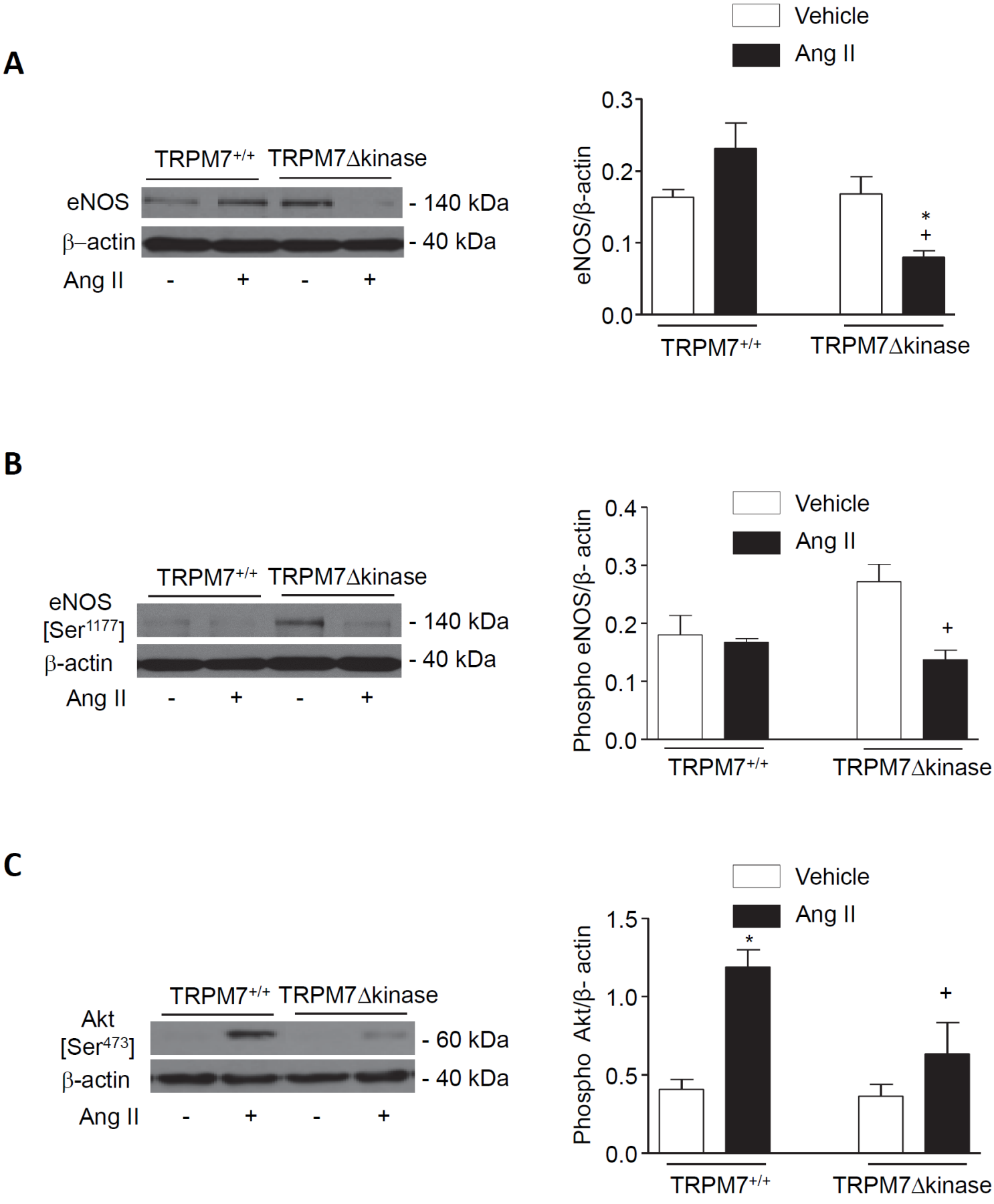
A
TRPM7+/+
TRPM7Δkinase
eNOS
- 140 kDa
β–actin
- 40 kDa
Ang II - + - +
Vehicle
Ang II
eNOS/β-actin
0.3
0.2
0.1
0.0
*
+
TRPM7+/+
TRPM7Δkinase
B
TRPM7+/+
TRPM7Δkinase
eNOS
[Ser1177]
- 140 kDa
β-actin
- 40 kDa
Ang II - + - +
Vehicle
Ang II
Phospho eNOS/β- actin
0.4
0.3
0.2
0.1
0.0
+
TRPM7+/+
TRPM7Δkinase
C
TRPM7+/+
TRPM7Δkinase
Akt
[Ser473]
- 60 kDa
β-actin
- 40 kDa
Ang II - + - +
Vehicle
Ang II
Phospho Akt/β- actin
1.5
1.0
0.5
0.0
*
+
TRPM7+/+
TRPM7Δkinase

Figure 6

A

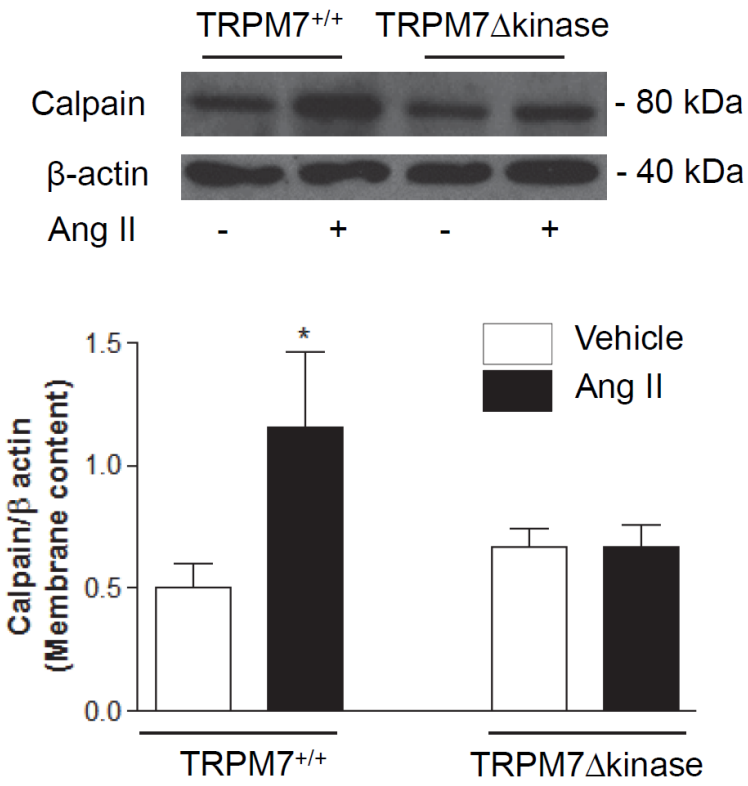
TRPM7+/+
TRPM7Δkinase
Calpain
- 80 kDa
β-actin
- 40 kDa
Ang II
-
+
-
+
Calpain/β actin (Membrane content)
1.5
1.0
0.5
0.0
*
Vehicle
Ang II
TRPM7+/+
TRPM7Δkinase

B

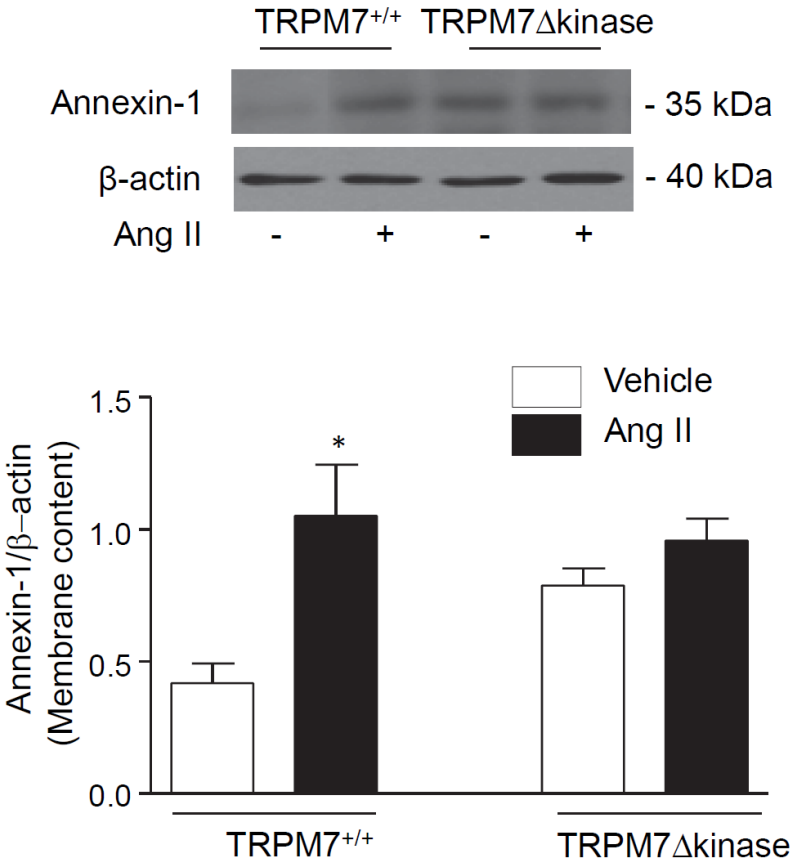
TRPM7+/+
TRPM7Δkinase
Annexin-1
- 35 kDa
β-actin
- 40 kDa
Ang II
-
+
-
+
Annexin-1/β–actin (Membrane content)
1.5
1.0
0.5
0.0
*
Vehicle
Ang II
TRPM7+/+
TRPM7Δkinase

Figure 7

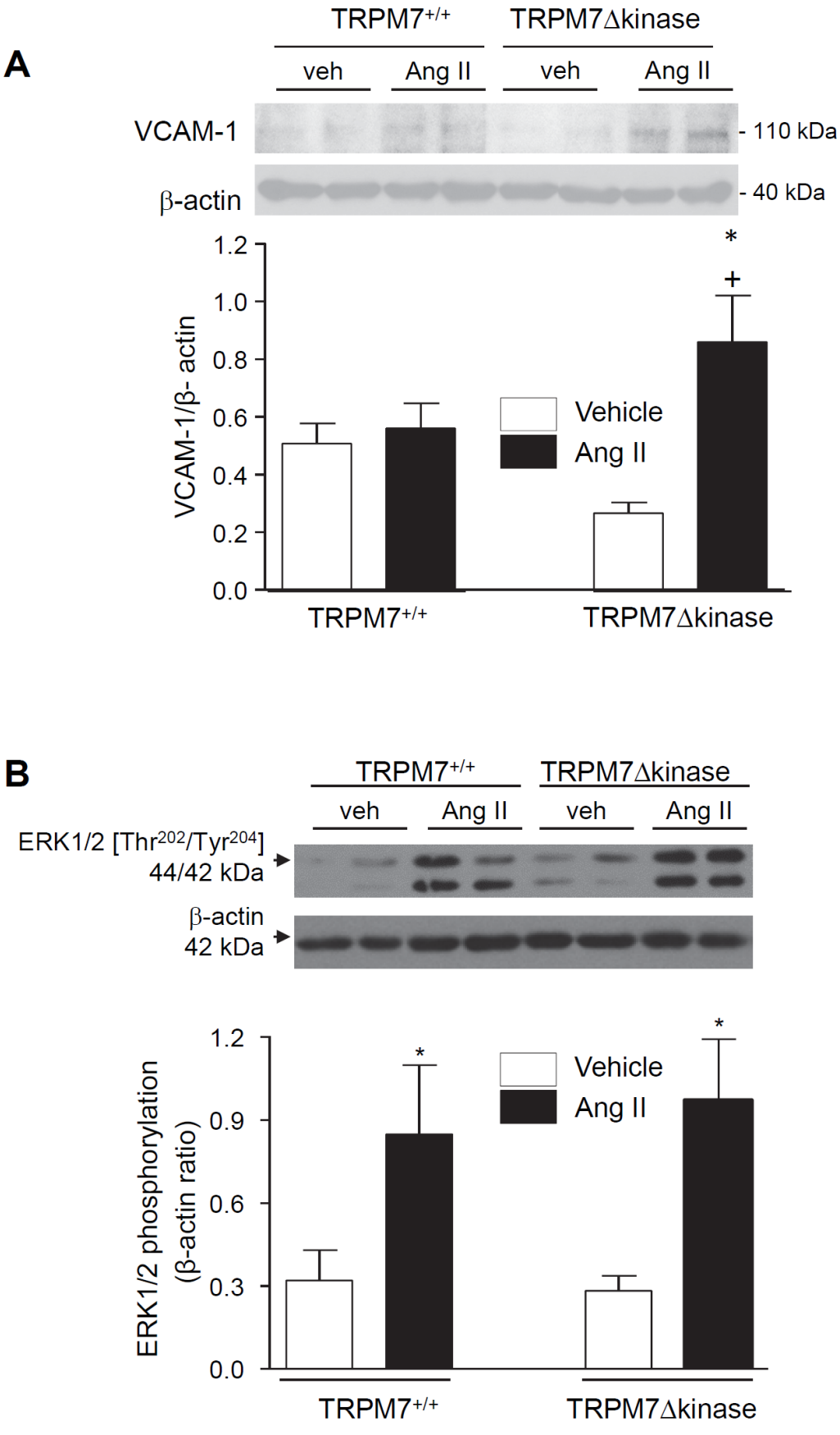
A
TRPM7+/+
TRPM7Δkinase
veh
Ang II
veh
Ang II
VCAM-1
- 110 kDa
β-actin
- 40 kDa
VCAM-1/β- actin
1.2
1.0
0.8
0.6
0.4
0.2
0.0
*
+
Vehicle
Ang II
TRPM7+/+
TRPM7Δkinase
B
TRPM7+/+
TRPM7Δkinase
veh
Ang II
veh
Ang II
ERK1/2 [Thr202/Tyr204]
44/42 kDa
β-actin
42 kDa
ERK1/2 phosphorylation
(β-actin ratio)
1.2
0.9
0.6
0.3
0.0
*
*
Vehicle
Ang II
TRPM7+/+
TRPM7Δkinase

Figure 8

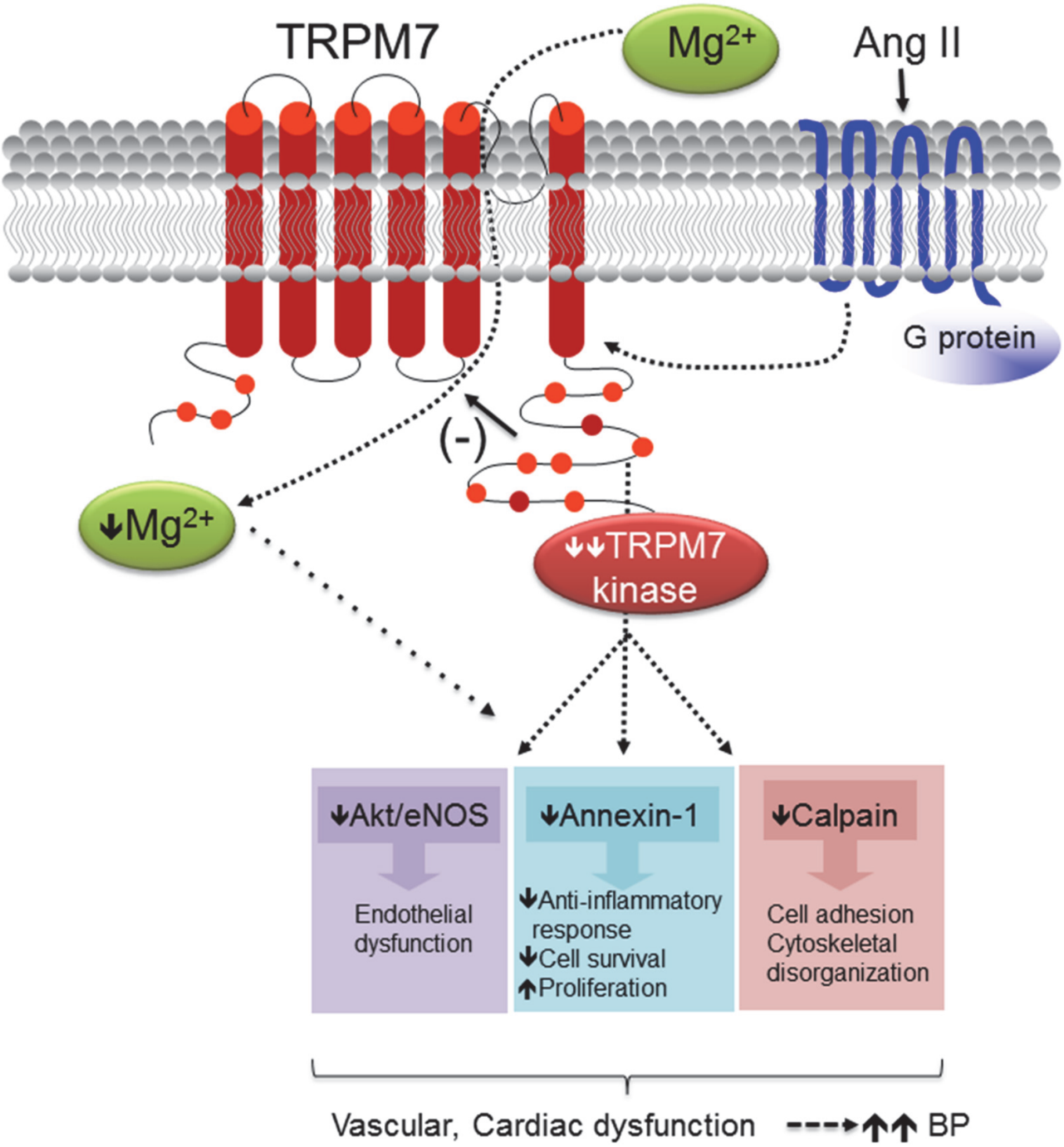
TRPM7
Mg2+
Ang II
G protein
(-)
↓Mg2+
↓↓TRPM7 kinase
↓Akt/eNOS
Endothelial dysfunction
↓Annexin-1
↓Anti-inflammatory response
↓Cell survival
↑Proliferation
↓Calpain
Cell adhesion
Cytoskeletal disorganization
Vascular, Cardiac dysfunction
↑↑ BP

Supplemental Text

Transient Receptor Potential Melastatin 7 Cation Channel (TRPM7) Kinase: a new player in hypertension

Tayze T Antunes[1], Glaucia E Callera[1], Ying He[1], Alvaro Yogi[1], Alexey G Ryazanov[2], Lillia V Ryazanova[2], Alexander Zhai[3], Duncan J Stewart[3], Alvin Shrier[4],

Rhian M Touyz[1,5].

[1]Kidney Research Centre, Department of Cellular and Molecular Medicine, Ottawa Hospital Research Institute, University of Ottawa, Canada;[2]Department of Pharmacology, Rutgers Robert Wood Johnson Medical School, USA;[3]Sprott Centre for Stem Cell Research and Regenerative Medicine Program, Dept. of Medicine, Ottawa Hospital Research Institute, University of Ottawa, Canada;[4]Department of Physiology and Groupe de Recherche Axé sur la Structure des Protéines, McGill University, Canada;[5]Institute of Cardiovascular & Medical Sciences, BHF Glasgow Cardiovascular Research Centre, University of Glasgow, UK.

To whom correspondence should be addressed:

Rhian M Touyz, MD, PhD

Institute of Cardiovascular and Medical Sciences,
BHF Glasgow Cardiovascular Research Centre, University of Glasgow,
126 University Place, Glasgow, G12 8TA
Phone: + 44 (0)141 330 7775/7774, Fax: + 44 (0)141330-3360,
Email: Rhian.Touyz@glasgow.ac.uk

Methods

Animals

The study was approved by the Animal Ethics Committee of the Ottawa Hospital Research Institute, University of Ottawa and carried out according to the recommendations of the Canadian Council for Animal Care. Male, 3 month old wild type ($TRPM7^{+/+}$) mice (C57BL/6J and SV129 background) and mice heterozygous for the deletion of the TRPM7kinase domain (TRPM7Δkinase), generated by the gene-targeting vector technique (1) were maintained in controlled room temperature (25°C) with a 12-h light/dark cycle and had free access to food and water. At 8 weeks of age, mice were infused with Ang II (400 ng/Kg/min) by osmotic minipumps for 4 weeks. Vehicle (saline)-infused mice were used as a control group. Systolic blood pressure (BP) was measured by tail-cuff plethysmography. Basal BP was measured on 3 different occasions before minipumps were surgically implanted in mice. After receiving the minipumps, BP was measured 1-2 times weekly. Spot urine samples were obtained a day prior to

sacrifice. At the end of the study, mice were killed by decapitation under anesthesia and mesenteric arteries, aorta, heart and blood samples collected for analysis.

Genotyping of TRPM7$^{+/+}$ and TRPM7Δkinase mice

A small piece of mouse ear was excised and DNA was extracted with a 100 µl of tissue extractor plus 25 µl of tissue preparation solution (REDExtract-N-Amp^{TM} Tissue PCR Kit, Sigma XNATR-1KT). Samples were incubated at room temperature for 10 minutes and then heated at 98 °C for 3 minutes, following by the addition of 100 µl of neutralizer. Samples were spun down and the supernatant obtained was kept at -20^{o}C for further PCR reaction. 4 µl of supernatant was used as a template in a 20 µl PCR reaction mix. Primers used to detect TRPM7kinase deletion (5' tgc gag gcc aga ggc cac ttg tgt agc 3'; and : 5' tgc gag gcc aga ggc cac ttg tgt agc 3') were designed to amplify the neighboring sequence regions of TRPM7kinase domain. Therefore, only in the absence of TRPM7kinase domain these primers were able to amplify the designated template during the PCR cycle specified. For this reason, when using these specificTRPM7 kinase primer set for genotyping TRPM7$^{+/+}$ mice, these samples do not show any product amplification since the extension time in our PCR conditions do not allow amplification of such a large sequence (TRPM7 plus neighbor sequence).

To guarantee that the absence of PCR bands with these primers were truly TRPM7$^{+/+}$ mice and not a result obtained due to a poor DNA extraction and/or PCR performance, a control primer set (5' aaa tct tag gct ggt aga cag tg 3'; and 5' ctt atc tct caa gcc aat tta gga g 3') independent of TRPM7kinase deletion was generated to accurately interpret the data. Therefore with the control primer set both TRPM7$^{+/+}$ and TRPM7Δkinase samples must show DNA amplification. PCR protocol was as following: 1 cycle of 94^{o}C (heat start), and 35 cycles of: 10 sec at 94^{o} C (denaturation), 30 sec at 62^{o} C (annealing), 2 min at 68^{o} C (extension). One final cycle of 5 min at 68^{o} C was performed, following by a hold on temperature of 4^{o} C. Agarose gel electrophoresis was used for visualizing the PCR products.

Validation of TRPM7kinase antibody in human embryonic kidney (HEK) cells expressing full length TRPM7 and in HEK cells deficient in TRPM7 mutant (Δ kinase)

Human TRPM7 WT and TRPM7 lacking a kinase domain (Δ kinase) cDNA cloning and the establishing of stable inducible expression of the corresponding proteins in HEK-293 T-Rex cells (Invitrogen) have been previously described (2). The stably transfected 293-HEK cells (expressing WT hTRPM7 and hTRPM7 Δ kinase under tetracycline control) were grown in in Dulbecco's Modified Eagle Medium (DMEM) containing 10% fetal bovine serum (FBS), 5 µg/ml Blasticidin S and 0.4 mg/ml Zeocin. Cells were grown in culture dishes treated with poly-Lysine (Sigma, P4832) in order to guarantee cell adherence once TRPM7 expression is induced upon addition of tetracycline. Briefly, to induce TRPM7 expression, cells were grown in the culture medium described above containing 1 µg/ml tetracycline for 24h. In the following day, cells were placed on starvation medium (DMEM containing 5 µg/ml Blasticidin S, 0.4 mg/ml Zeocin) and 1 µg/ml tetracycline overnight. Analysis of TRPM7 expression was performed by Western blotting using TRPM7 antibody (Epitomics Abcam, Rabbit mAb # 3828-1) (described below) in control cells (without tetracycline treatment) and in cells exposed to tetracycline to induce gene expression (48h).

Biochemical analysis

Plasma was collected immediately following sacrifice and kept at -80°C until further analysis. Electrolyte, cholesterol, urea, glucose, creatinine, and protein concentrations were determined using an automated analyzer (Beckman Coulter AU5800) by IDEXX Laboratories (Ontario, Canada).

Urinary nitric oxide measurement

Spot urine was kept at -80°C until further analysis. Total nitrate/nitrite levels were measured in the urine as nitric oxide metabolites using the Nitrate/Nitrite Colorimetric Assay Kit (Cayman Chemical, Ann Arbor, USA).

Urinary Albumin and Creatinine measurement

Assessment of albumin (µg/mL) and creatinine (mg/mL) excretion was performed in urine samples with commercial kits (Albuwell M and Creatinine Companion, Exocell) according to the manufacturer's instructions. Results were expressed as albumin:creatinine ratio (ACR).

Echocardiography

Cardiac geometry and function were performed using a Vevo 2100 imaging system with a 40-MHz transducer. Vehicle and Ang II-infused TRPM7$^{+/+}$ and TRPM7Δkinase mice were analyzed at the end of the study (25-27 days following Ang II infusion). Mice were lightly sedated by continuous gas inhalation (isoflurane, 1.5-2%) throughout the examination. Mice were secured in the supine position on a warming pad, the chest hair was shaved, and a warmed echo gel was placed on the shaved chest. Echo images were downloaded afterwards and analyzed offline using the Vevo 2100 software. 7 beats were measured for each mouse and averaged for the interpretation of any given measurements. For all the measurements shown, the hearts were examined in M-mode in the parasternal long axis view. All calculated parameters were automatically computed by the Vevo 2100 standard measurement package as previously reported (3).

Histological analyses

For histological and immunohistochemical analyses, the heart and aorta were fixed in 4 % paraformaldehyde and processed for paraffin embedding. Sections (5 µm thick) were stained with Sirius Red and Masson's Trichrome. Hematoxylin and eosin staining was performed for LV wall analysis as well as heart's gross morphology. For the morphometric analysis in cross-sections of heart, the left ventricle wall was measured in three regions and the values were averaged. Sirius red staining was performed to examine collagen deposition and Masson's trichrome to determine fibrosis.

For morphometric analysis in cross-sections of aorta, wall thickness was measured in four regions and the values were averaged. For immunohistochemical staining in aorta sections, heat-induced epitope retrieval was performed at 110^{o} C for 12 min with tris-EDTA buffer (pH 9.0). To localize TRPM7, anti-TRPM7-C-terminal (#135817, Abcam, Cambridge, UK) primary antibody (dilution 1/50, rabbit) was used. The specificity of the staining was determined upon absence of immunoreactivity when the primary antibody was omitted.

Wire myography to assess vascular function

Vascular function in second order branches of mesenteric resistance arteries were studied with a wire myograph (DMT, Danish Myo Technology, Denmark) as previously described (4). Mesenteric resistance arteries were placed in Krebs Henseleit solution (mM: 118 NaCl, 4.65 KCl, 1.18 $MgSO_4$, 1.18 KH_2PO_4, 25 $NaHCO_3$, 2.5 $CaCl_2$, 0.026 EDTA, and 5.5 glucose) under a

dissecting microscopy, carefully cleaned of connective tissue, and second order branches (corresponding with resistance arteries) were isolated and mounted. Arterial segments (≤ 2 mm long) were cannulated by threading them onto two stainless steel wires (25 μm) and tying the wires to two supports. Arteries were continuously bubbled with 95% O_2 and 5 % CO_2 to achieve a pH of 7.4 at 37°C, allowed to equilibrate for 20 minutes, and normalized prior to experiments. Vessel contractility was accessed by cumulative concentration-response curves (10^{-9} to 3 x 10^{-5} M) to norepinephrine (NE). Endothelium-dependent and -independent relaxation was assessed by measuring dilatory responses to cumulative concentration-response curves (10^{-9} to 3 x 10^{-5} M) of acetylcholine (ACh) and diethylamine NONOate (DEA-NO), respectively, in vessels pre-contracted with NA at a concentration to achieve approximately 80% of maximal response.

Pressure myography to assess vascular structure and mechanics

Structural and mechanical properties of mesenteric resistance arteries were studied with a pressure myograph (Living Systems, Burlington, Vermont) (4,5). Mesenteric resistance arteries were placed in Krebs Henseleit solution, cleaned and dissected as described above. Arterial segments (2 to 3 mm long) were slipped onto 2 glass microcannulae, one of which was secured until the vessel walls were parallel, set to a pressure of 45 mmHg and allowed to equilibrate for 30-60 min at 37 °C in a calcium-free Krebs Henseleit solution (with the addition of 10 mM EGTA) to eliminate myogenic tone. Arteries were gassed with a mixture of 95 % O_2 and 5 % CO_2 at 37°C. Lumen diameter and vessel thickness were measured during a pressure-diameter curve by increasing intraluminal pressure in 20 mmHg steps between 0 and 120 mmHg. Lumen diameter, cross-sectional area, media to lumen ratio (structure), stress, strain and mechanics were calculated as previously reported (3, 4).

Vascular tissue preparation for Western Blotting analysis

Total protein was extracted from vascular homogenates. Frozen aortas and mesenteric arteries were homogenized in 50 mM Tris-HCl (pH 7.4) lysis buffer (containing 1% Nonited P-40, 0.5% sodium deoxycholate, 0.1% SDS, 2 mM Na_3VO_4, 1 mM phenylmethylsulfonyl fluoride (PMSF), 1μg/mL pepstatin A, 1 μg/mL leupeptin and 1 μg/mL aprotinin). Protein supernatant was separated by centrifugation at 13,000 x g for 10 min and pellet was discarded. The particular supernatant was kept at -80°C.

Mesenteric resistance arteries were fractionated to obtain cytosol and membrane-enriched fractions. Frozen mesenteric resistance arteries were pulverized (TP-103 Amalgamator) in 80 ul of cold buffer A, which consisted of 50 mM Tris-HCl pH 7.4, 2.5 mM EDTA, 5 mM EGTA, 2 mMNa_3VO_4, 1 mM PMSF, 1 μg/ml leupeptin, 1 μg/ml aprotinin and 1 μg/ml pepstatin. The homogenate was centrifuged at 100,000 x *g* for 60 min at 4°C (ultracentrífuge Optima MAX (Beckman Coulter, CA, EUA), thereby isolating the cytosolic fractions in the supernatant. The pellet was resuspended in lysis buffer B; which consisted of lysis buffer A with the addition of 1% triton X-100; homogenized again, and centrifuged at 13,000 *g* for 10 min at 4°C. The supernantant obtained contained the membrane fractions. The cytosolic and membrane fractions obtained were kept at -80°C.

Western Blotting

Total protein from aorta homogenates (30 μg), mesenteric arteries (25 μg) and membrane-enriched fractions (4 μg) from mesenteric arteries were used for Western Blot analysis. Proteins were separated by electrophoresis on a polyacrylamide gel (10%), and transferred onto a

nitrocellulose membrane. Nonspecific binding sites were blocked with 5% skim milk in Tris-buffered saline solution with 0.1% Tween for 1 hour at room temperature. Membranes were then incubated with specific antibodies overnight at 4°C. Antibodies were as follows: TRPM7 (Epitomics, Abcam, Burlingame, CA); annexin-1, calpain, caveolin-1, VCAM-1, p47 phox (Santa Cruz Biotechnology, Dallas, Texas); phospho-JNK, phospho-ERK1/2, phospho Akt, phospho eNOS and eNOS (Cell Signaling, Danvers, MA). With the exception of VCAM-1 (1:500) and TRPM7 (1:250), all the antibodies were used in a 1:1000 dilution. β-actin (1:5000 dilution; Sigma, Oakville, ON) was used as an internal housekeeping control. After incubation with secondary antibodies, signals were revealed with chemiluminescence, visualized by autoradiography and quantified densitometrically.

Reactive Oxygen Species (ROS) Assessment

Vascular ROS generation was measured by lucigenin-enhanced chemiluminescence assay, with lucigenin as the electron acceptor and NADPH as the substrate. Aortic segments from $TRPM7^{+/+}$ and TRPMΔkinase mice treated with Ang II or vehicle were homogenized in assay buffer (50 mmol/L of KH_2PO_4, 1 mmol/L of EGTA, and 150 mmol/L of sucrose, pH 7.4) with a glass-to-glass homogenizer. The assay was performed with 100 µL of sample, 1.25 µL of lucigenin (5 µmol/L), 25 µL of NADPH (0.1 mmol/L) and assay buffer to a total volume of 250 µL. Luminescence was measured for 20 cycles of 18 seconds each by a luminometer (Lumistar Galaxy, BMG Lab Technologies, Germany). Basal readings were obtained prior to the addition of NADPH to the assay. The reaction was initiated by the addition of the substrate. Basal and buffer blank values were subtracted from the NADPH-derived luminescence. Superoxide anion production was expressed as relative luminescence unit (RLU)/µg protein.

Plasma hydrogen peroxide (H_2O_2) was assessed with Amplex Red assay kit (Molecular Probes by Invitrogen). H_2O_2 was detected spectrophotometrically in 10 µL of plasma sample. Absorbance was measured at multiple time points (0 to 60 min).

References

1. Ryazanova LV, Rondon LJ, Zierler S, Hu Z, Galli J, Yamaguchi TP, Mazur A, Fleig A, Ryazanov AG. TRPM7 is essential for Mg(2+) homeostasis in mammals. *Nat Commun.* 2010;1:109-113.
2. Yogi A, Callera GE, O'Connor S, Antunes TT, Valinsky W, Miquel P, Montezano AC, Perraud AL, Schmitz C, Shrier A, Touyz RM.Aldosterone signaling through transient receptor potential melastatin 7 cation channel (TRPM7) and its α-kinase domain. *Cell Signal.* 2013;25:2163-2175.
3. Vinhas M, Araújo AC, Ribeiro S, Rosário LB, Belo JA. Transthoracic echocardiography reference values in juvenile and adult 129/Sv mice. *Cardiovasc Ultrasound*. 2013;11:12-14
4. Briones AM, Nguyen Dinh Cat A, Callera GE, Yogi A, Burger D, He Y, Corrêa JW, Gagnon AM, Gomez-Sanchez CE, Gomez-Sanchez EP, Sorisky A, Ooi TC, Ruzicka M, Burns KD, Touyz RM. Adipocytes produce aldosterone through calcineurin-dependent signaling pathways: implications in diabetes mellitus-associated obesity and vascular dysfunction. *Hypertension*. 2012;59:1069-1078.

5. Endemann D, Touyz RM, Li JS, Deng LY, Schiffrin EL. Altered angiotensin II-induced small artery contraction during the development of hypertension in spontaneously hypertensive rats. *Am J Hypertens*. 1999;12:716-723.

Figure legends

Supplemental figure S1. Hematoxylin and eosin staining of the heart of Ang II-infused TRPM7$^{+/+}$ and TRPM7Δkinase mice. Hearts were isolated from TRPM7$^{+/+}$ and TRPM7Δkinase mice infused with vehicle or Ang II (400 ng/Kg/min). (A) Panels are representative photomicrographs of paraffin-embedded heart sections of 8-10 mice per group processed for hematoxylin and eosin staining with original magnification of x5, scale bar 200 μm. (B) For the morphometric analysis of left ventricle (LV) wall size, the LV wall thickness was measured in three regions and the values were averaged. Results are presented as mean ± SEM of 8-10 mice per group. $^{*}p<0.05$ vs vehicle-infused TRPM7Δkinase mice.

Supplemental figure S2. Collagen accumulation and interstitial fibrosis in the heart of Ang II-infused TRPM7$^{+/+}$ and TRPM7Δkinase mice. Hearts were isolated from mice infused with vehicle or Ang II. Panels are representative photomicrographs of paraffin-embedded of heart sections of 8-9 mice per group processed for Sirius Red (A) and Masson's trichrome (B) and, with original magnification of x20, scale bar 20 μm. Insets depict collagen accumulation (A) and fibrosis (B) of the arteries.

Supplemental figure S3. Aortic hypertrophy in Ang II-infused mice. Aortas were isolated from TRPM7$^{+/+}$ and TRPM7Δkinase infused with vehicle or Ang II. Paraffin-embedded thoracic aorta sections were processed for Masson's trichrome staining. For the morphometric analysis in cross-sections of aorta, the wall thickness was measured in four regions and the values were averaged. Upper panels, representative photomicrographs of Masson's trichrome-stained thoracic aorta sections, with original magnifications x200. Bar graph, wall thickness of aortic segments. Results are presented as mean ± SEM of 6-7 mice per group.*P <0.05 vs. respective vehicle-infused mice.

Supplemental figure S4. Structural changes in mesenteric arteries from Ang II-infused TRPM7$^{+/+}$ and TRPM7Δkinase mice. Mesenteric arteries were isolated from TRPM7$^{+/+}$ and TRPM7Δkinase mice infused with vehicle or Ang II and mounted as pressurized systems. Lumen diameter (A), media cross-sectional area (B), and media lumen ratio (C) were analyzed by pressure myography. Mesenteric arteries were incubated in 0 Ca^{2+} physiological salt solution containing 10 mmol/L EGTA and were subjected to increasing levels of intraluminal pressure as indicated. Line graphs represent mean ± SEM of 5 mice per group. *p<0.05 vs vehicle-infused counterparts.

Supplemental figure S5. Expression of eNOS and caveolin-1 in membrane-enriched vascular fractions from Ang II-infused TRPM7$^{+/+}$ and TRPM7Δkinase mice. Mesenteric arteries were isolated from TRPM7$^{+/+}$ and TRPM7Δkinase mice infused with vehicle or Ang II. Protein expression of eNOS (A) and caveolin-1 (B) was analyzed in membrane-enriched fractions. Data are presented as the expression of eNOS (A) and caveolin-1 (B) relative to the expression of β-actin. Results are presented as mean ± SEM of 5-9 mice per group. *p<0.05 vs vehicle-infused TRPM7$^{+/+}$: $^{+}p<0.05$ vs Ang II-infused TRPM7$^{+/+}$.

Supplemental figure S6. Ang II effects on JNK phosphoryltion in aortas. Aortas were isolated from TRPM7$^{+/+}$ and TRPM7Δkinase mice infused with vehicle or Ang II.

Phosphorylation levels of JNK are presented relative to expression of β actin. Upper panels, representative immunoblots of phospho-JNK and β-actin. Results are presented as mean ± SEM of 5-9 mice per group. *$p<0.05$ vs vehicle-infused counterparts.

Supplemental figure S7. Vascular and systemic oxidative stress in Ang II-infused TRPM7$^{+/+}$ and TRPM7Δkinase mice. Plasma, aorta, and mesenteric arteries were obtained from TRPM7$^{+/+}$ and TRPM7$^{+/-}$ mice infused with vehicle or Ang II. (A) plasma H_2O_2 status accessed by Amplex red following a 30 min reaction time; (B) time-course of Amplex red reaction (0 to 60 min). (C) Superoxide anion generation accessed in aorta homogenates by lucigenin-enhanced chemiluminescence. (D) Protein expression of p47phox analyzed in membrane-enriched fractions and presented as a ratio to β actin. Upper panels, representative immunoblots of p47phox and β actin. Bar and line graphs represent mean ± SEM of 5-14 mice per group.

Supplemental Figure S1

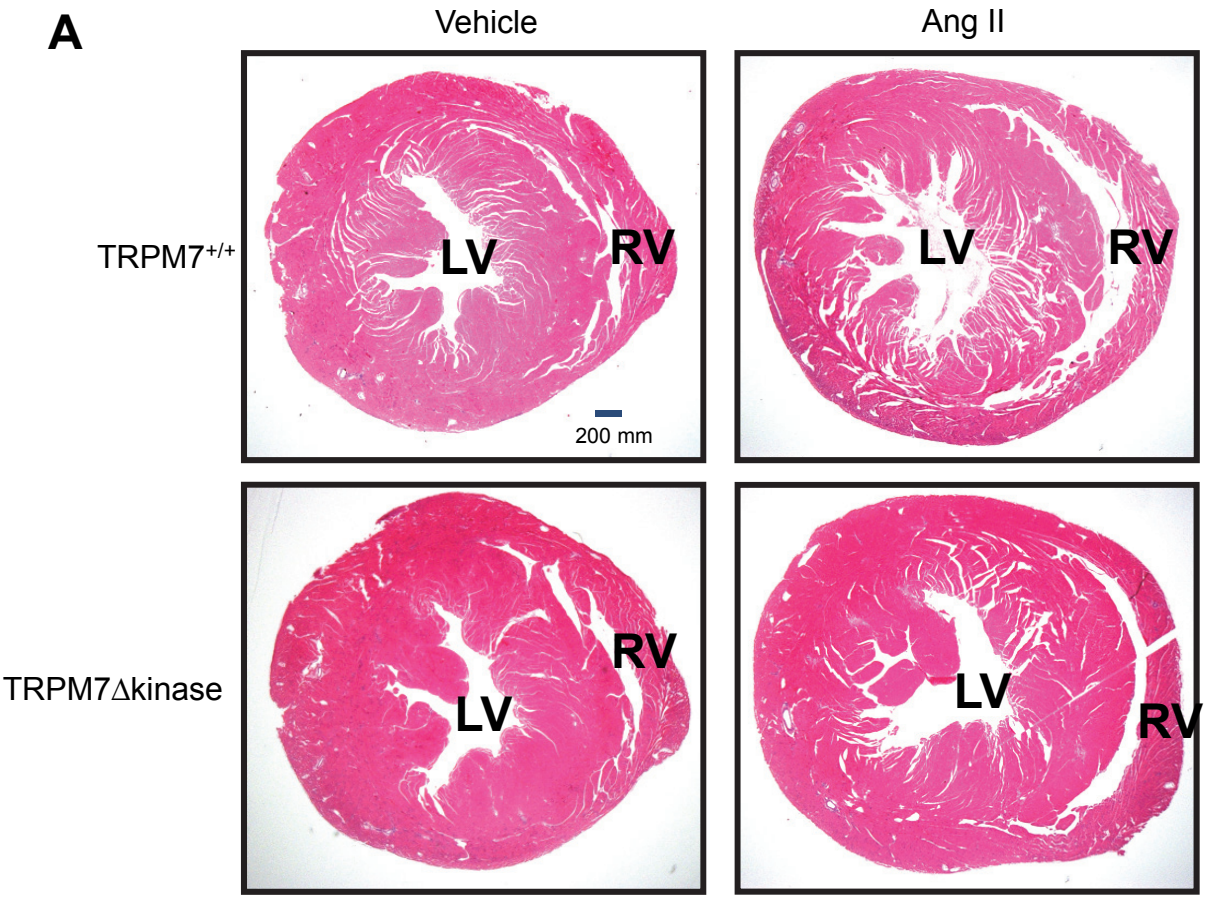

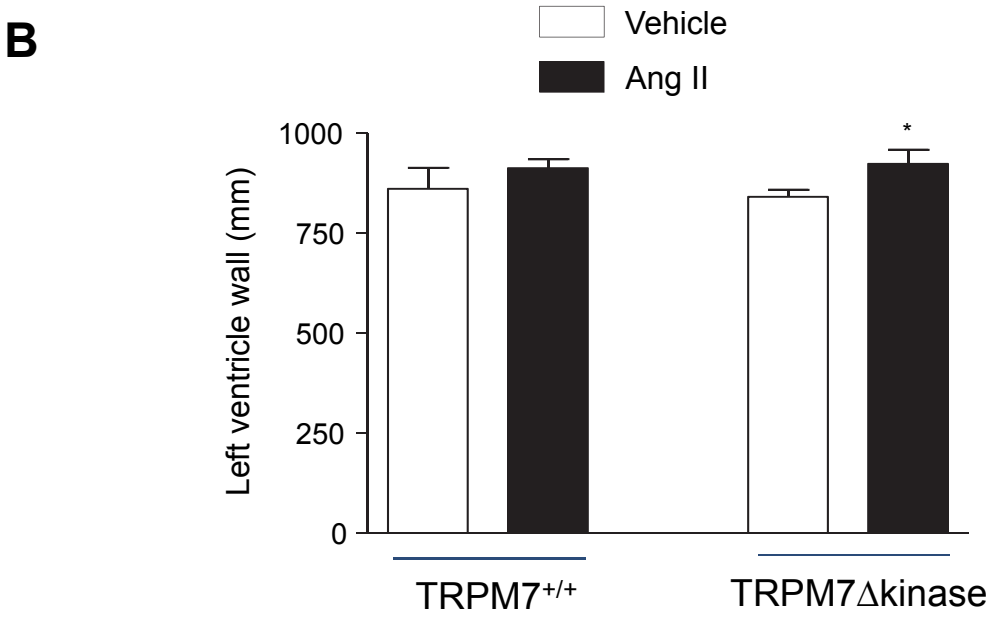

Supplemental Figure S2

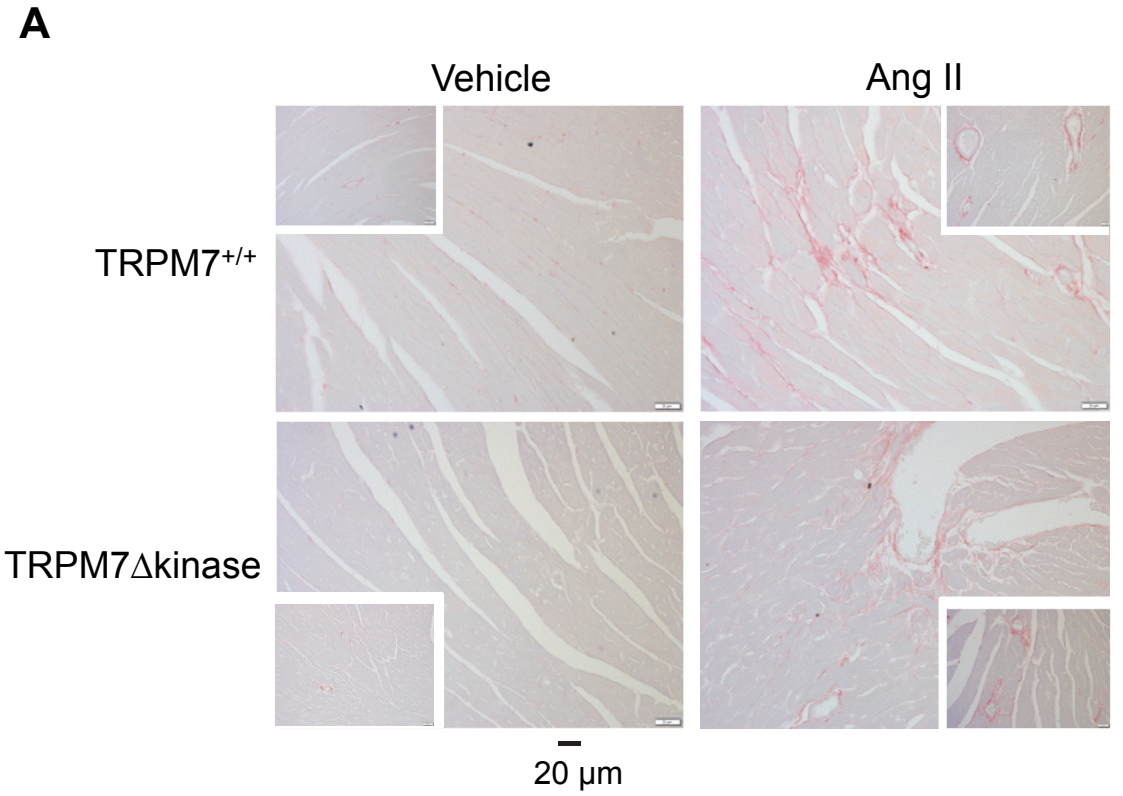

Supplemental Figure S3

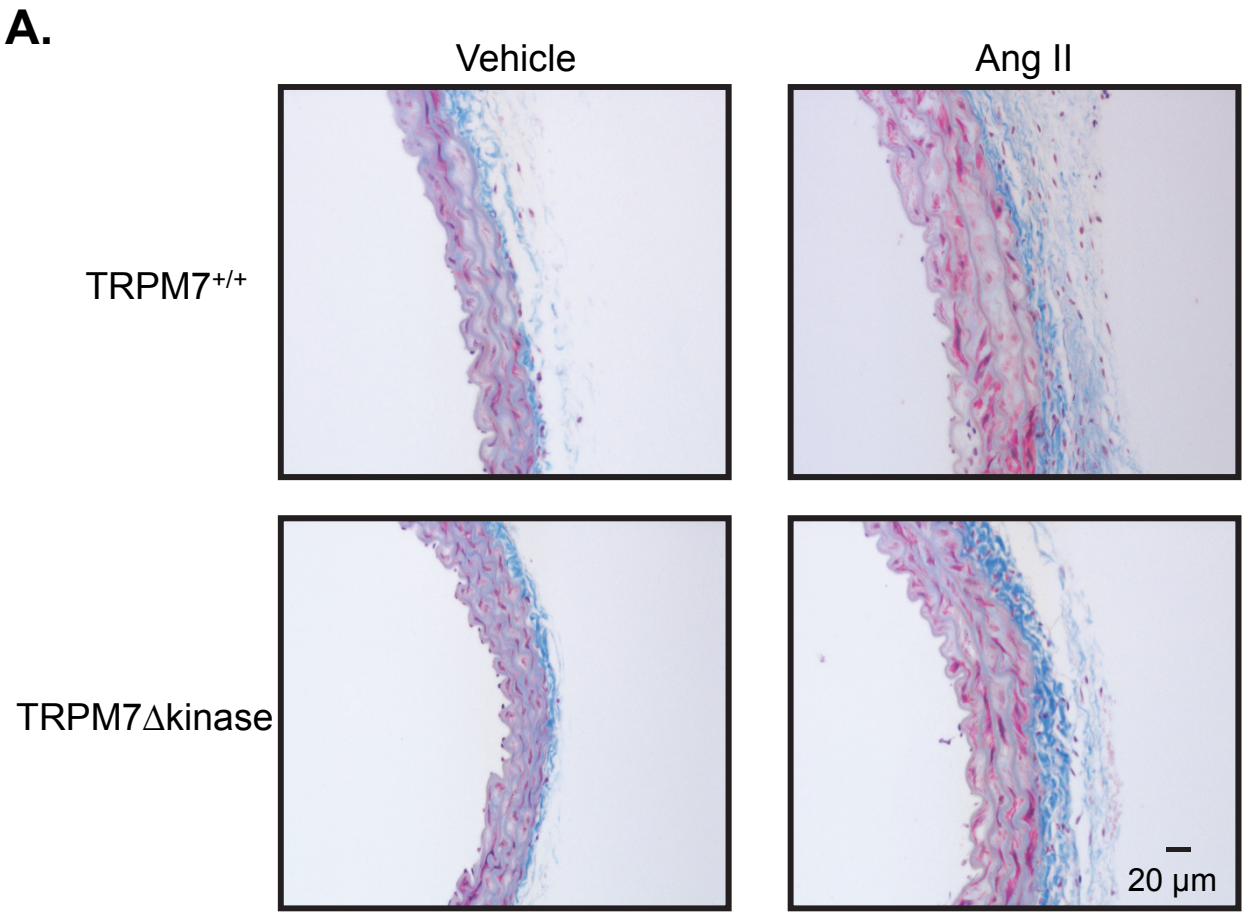

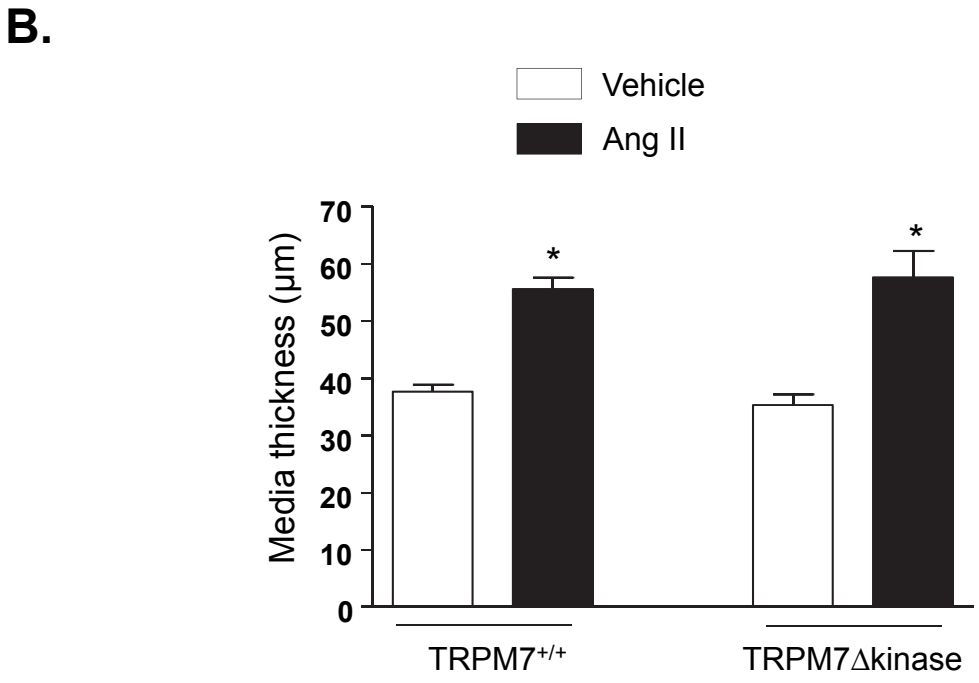

Supplemental Figure S4

A.

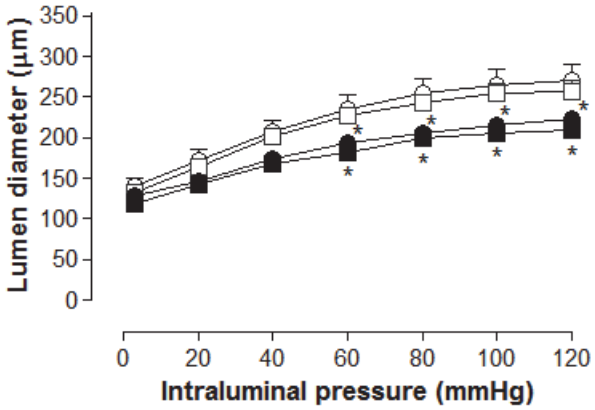

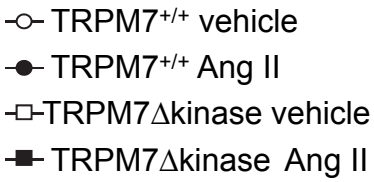

B.

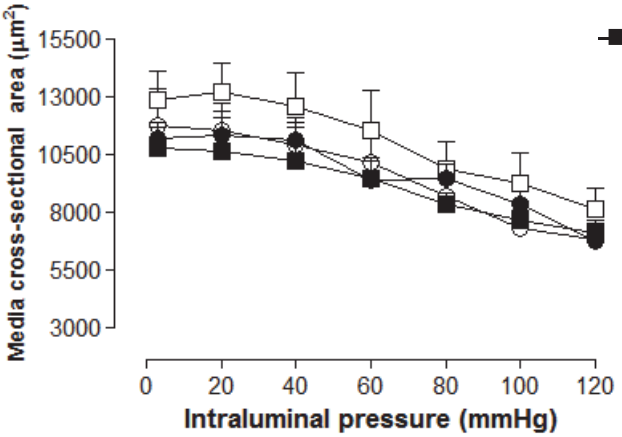

C.

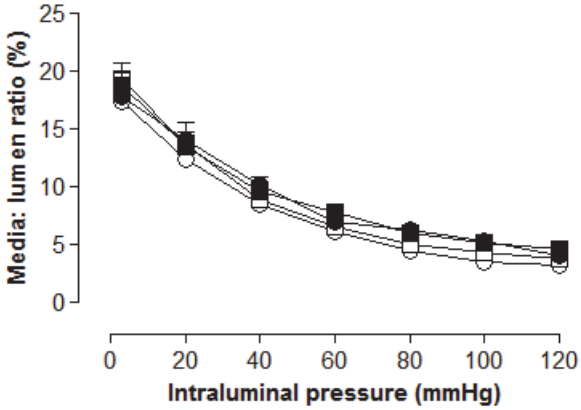

Supplemental Figure S5

A

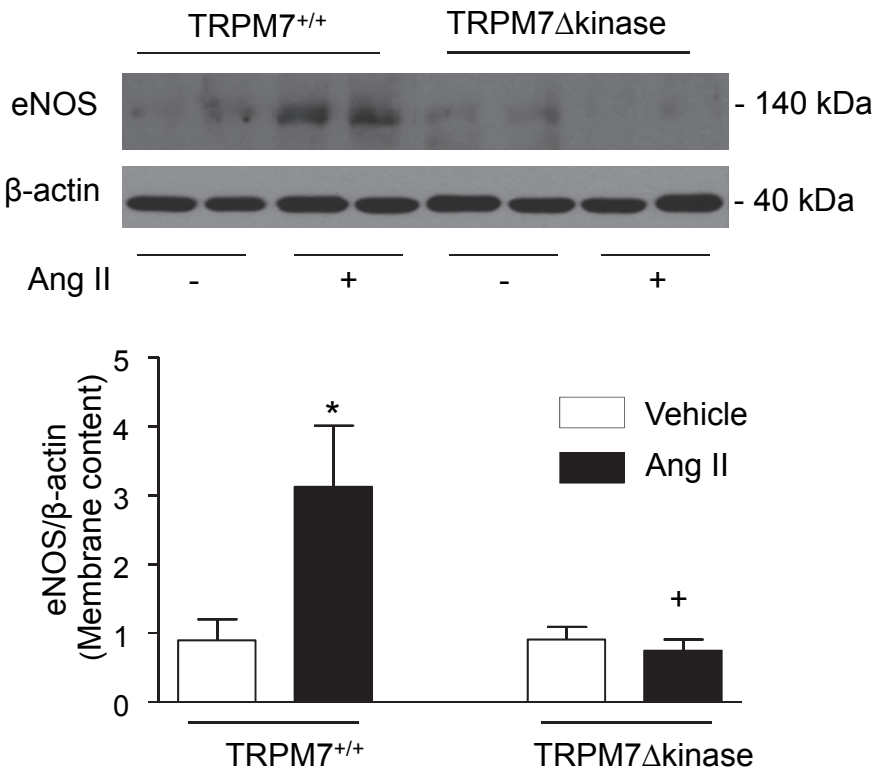

B

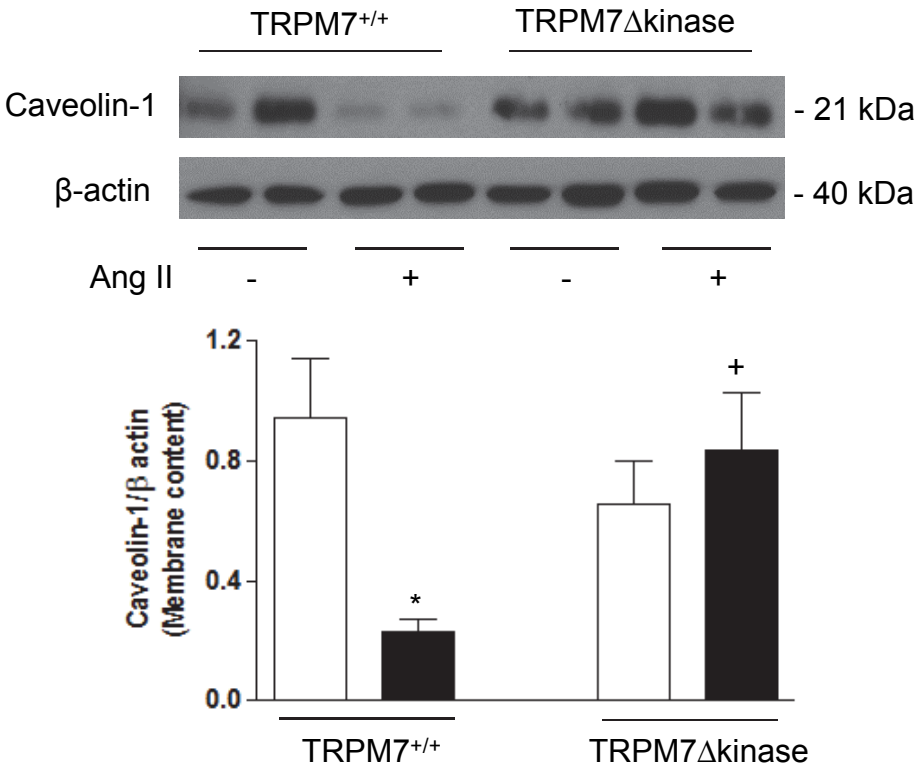

Supplemental Figure S6

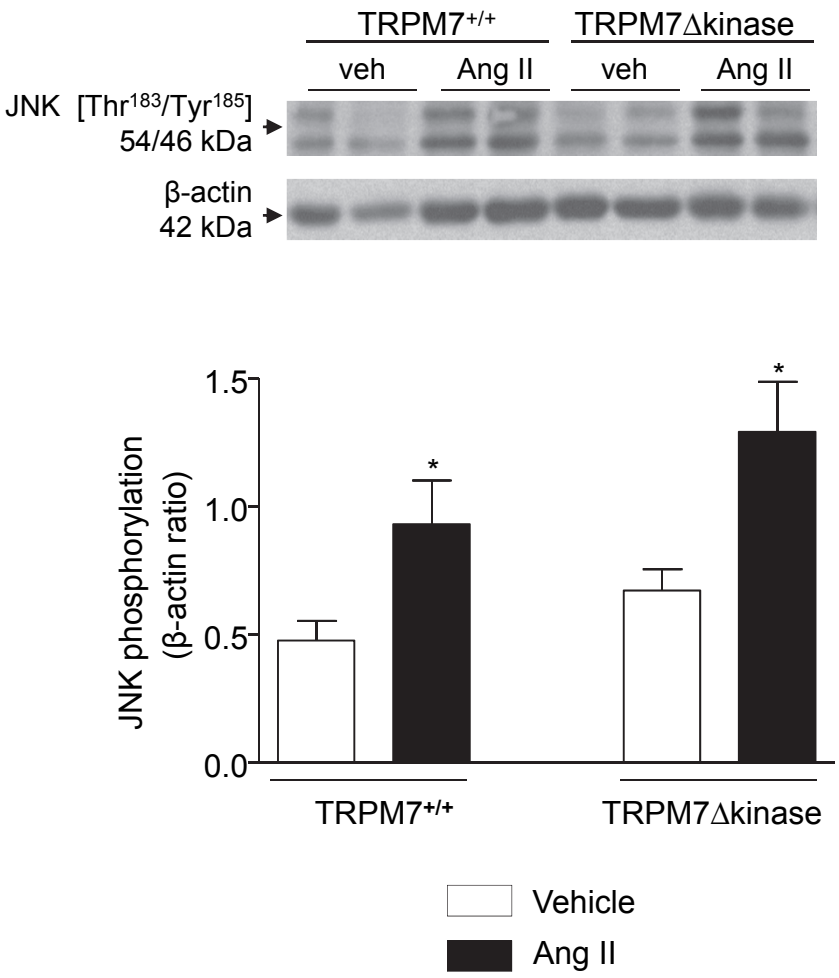

Supplemental Figure S7